Evaluation of methods to characterise the geochemistry of limestone and its fracturing in connection to heating

Jessica Jennerheim

Dissertations in Geology at Lund University,
Master's thesis, no 486
(45 hp/ECTS credits)

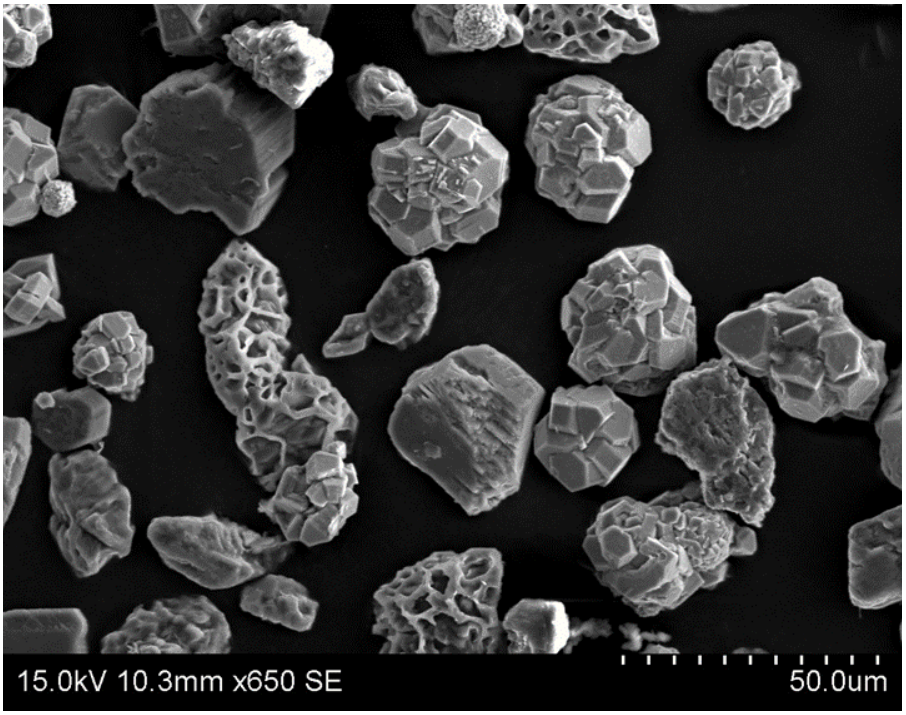

Department of Geology
Lund University
2016

Evaluation of methods to characterise the geochemistry of limestone and its fracturing in connection to heating

Master's thesis

Jessica Jennerheim

Department of Geology
Lund University
2016

Contents

1 Introduction **8**
2 Background **8**
2.1 Location 8
2.2 Depositional environments of carbonates 8
2.3 Chemical properties of limestones 11
2.4 The sedimentary bedrock of Gotland 11
2.4.1 Chemical properties of the Slite Group 13
2.4.2 Chemical properties of the Storugns limestone 13
2.5 The formation of fines 13
3 Methods **14**
3.1 Core logging and cutting 14
3.2 XRF 14
3.3 Handheld XRF 14
3.4 Computer analysis 15
3.5 Students t-test 15
3.6 SEM 15
4 Results **15**
4.1 Logging 15
4.2 ITRAX - Geochemistry 17
4.2.1 Major elements 17
4.2.2 Trace elements 20
4.3 Geochemistry of the rock types 20
4.3.1 Marl /marlstone 20
4.3.2 Calcilutite 21
4.3.3 Calcarenite 22
4.3.4 Stromatoporoid limestone 23
4.3.5 Fragment limestone 24
4.3.6 Reef limestone 25
4.4 Handheld XRF 26
4.5 Student's t-test 26
4.6 SEM 27
5 Discussion **28**
5.1 Chemistry 28
5.1.1 Major elements 28
5.1.2 Trace elements 28
5.1.3 Geochemistry of the rock types 28
5.1.3.1 Marl/marlstone 28
5.1.3.2 Calcilutite 28
5.1.3.3 Calcarenite 29
5.1.3.4 Stomatoporoid limestone 29
5.1.3.5 Fragment 29
5.1.3.6 Reef 29
5.2 Handheld XRF 29
5.3 Student's t-test 29
5.4 SEM 30
6 Sources of error **30**
7 conclusions 30
Part 2 ..... **31**
1 Introduction **31**
2 Background **31**

Cover picture: SEM image of the residual minerals after dissolving a sample in acetic acid.

2.1 Thermal properties of limestone 31
3 Method 32
3.1 Drilling and cutting 32
3.2 X-ray computed tomography 32
3.2.1 Setup and theory 32
3.2.2 Data visualisation 32
3.2.3 CT in geology 33
3.3 CT to find dolomite 33
3.3.1 Acid test & handheld XRF 33
3.3.2 SEM 33
3.4 CT to characterise fractures 33
4 Results 34
4.1 CT to find dolomite 34
4.1.1 Acid test & handheld XRF 34
4.4.2 SEM 34
4.4.3 CT 35
4.5 CT to characterise fractures 35
4.5.1 Heated to 400 degrees 35
4.5.2 Heated to 500 degrees 35
4.5.3 Heated to 600 degrees 35
4.5.4 Heated to 650 degrees 36
4.5.5 Heated to 700 degrees 37
5 Discussion 38
5.1 Acid test 38
5.2 CT to find dolomite 38
5.3 CT to characterise fractures 38
6 Sources of error 39
7 Conclusions 39
8 Acknowledgement 39
9 References 39
Appendix 41

Evaluation of methods to characterise the geochemistry of limestone and its fracturing in connection to heating

JESSICA JENNERHEIM

Jennerheim, J., 2016: Evaluation of methods to characterise the geochemistry of limestone and its fracturing in connection to heating *Dissertations in Geology at Lund University*, No. 486. 50pp. 45 hp (45 ECTS credits) .

Abstract: In 2011 Vinnova funded a joint project between Nordkalk AB, Kalkproduktion Storugns AB (KPAB) and the department of Geology at the University of Lund. The goal of the project is to increase the general knowledge of limestone and in extension, facilitate for the industry. This thesis is a part of the project and consists of two separate parts which look into the geochemistry and thermal properties of limestones. Part one focuses on a 29 m drill core from the Storugns quarry on Gotland consisting of calcarenite, calcilutite, marl/marlstone, stromatoporoid, fragment and reef limestone. The drill core was scanned with a high resolution XRF (ITRAX) and the geochemistry between the different types of limestones was compared. Focus ended up on silica (SiO_2) and calcium oxide (CaO) as they were the most common elements in the core and a statistical comparison using a student's t-test was conducted. To get comparable data to other studies from the area, a handheld XRF was used on polished and cut parts of the core which represent the different types of limestone (except the marl/marlstone). Samples from each rock type (again except the marl/marlstone) were dissolved in acetic acid and the residual material was analysed in a SEM, more specifically using EDS. The results show that beside calcite and dolomite, the rock mostly contain pyrite and quartz. The ITRAX scan confirms that geochemistry varies between the rock types, especially when looking at the CaO and SiO_2. Therefore, the ITRAX scan was deemed a reliable method to distinguish different types of limestone whereas the handheld XRF was not. Part two of the thesis focuses on the thermal properties of limestone and more specifically if x-ray computed tomography (CT) is a viable method for distinguishing dolomite from calcite and if it can be used to study heat related fractures. Four samples were collected from the Storugns quarry on Gotland and after drilling six cores per sample, the sample containing the most magnesium was determined by using an acid test, handheld XRF and SEM (EDS). Five cores from this sample were scanned with a CT. After scanning, the cores were heated to 400, 500, 600, 650 and 700 °C respectively and then scanned in the CT again. Using a program called Fiji ImageJ, five levels were chosen in the images from the unburnt samples and the corresponding levels were located in the burnt cores' images. The images were then compared and all fractures were marked and measured. The results show that CT is a good method for studying fractures however additional studies would be needed to modify the method in order to use it to distinguish dolomite from calcite.

Keywords: geochemistry, limestone, Gotland, thermal properties, x-ray fluorescence, x-ray computed tomography

Supervisor(s): Leif Johansson, Mikael Erlström

Jessica Jennerheim, Department of Geology, Lund University, Sölvegatan 12, SE-223 62 Lund, Sweden. E-mail: nat11jje@student.lu.se

Utvärdering av metoder för att karaktärisera geokemin i kalksten och dess sprickbildning i relation till upphettning

JESSICA JENNERHEIM

Jennerheim, J., 2011: utvärdering av metoder för att karaktärisera geokemin i kalksten och dess sprickbildning i relation till upphettning. *Examensarbeten i geologi vid Lunds universitet*, No. 486, 50 pp. 45 hp (45 ECTS credits)

Sammanfattning: År 2011 finansierade Vinnova ett projekt som är ett sammarbete mellan Nordkalk AB, Kalkproduktion Storugns AB (KPAB) och Geologiska Institutionen vid Lunds universitet. Målet med projektet är att ge en ökad kunskap om kalksten och i förlängning underlätta för industrin. Detta mastersarbete är en del av projektet och består av två separata delar. Del ett fokuserar på en 29 m lång borrkärna från Storugns stenbrott på Gotland. Borrkärnan består av kalkarenit, kalcilutit, märgel/märgelsten, stromatoporoidé-, rev- och fragmentkalksten. Först scannades kärnan i hög upplösning med en XRF (ITRAX) och därefter jämfördes geokemin mellan de olika typerna av kalksten. Fokus lades på kiseldioxid (SiO_2) och kalciumoxid (CaO), då de var de mest vanligt förekommande ämnena i kärnan, och en statistisk jämförelse mellan kalkstenstyperna gjordes med ett t-test. För att få data som är jämförbara med tidigare undersökningar av platsen analyserades delade och polerade bitar av kärnan som representerar de olika kalkstenstyperna (förutom märgel/märgelsten) med en handhållen XRF. Prov från alla kalkstenstyper (igen bortsett från märgel/märgelsten) löstes upp i ättiksyra och residual-materialet analyserades med en SEM, närmare bestämt EDS. Resultaten visar att borrkärnan mest innehåller pyrit och kvarts, om man bortser från kalcit och dolomit. ITRAX-scanning bekräftar att geokemin varierar mellan kalkstenstyperna, särskilt om CaO och SiO_2 undersöks. ITRAX-scanning bedöms därför vara en god metod att särskilja kalkstenstyper med medan den handhållna XRF inte bedöms vara det. Del två av masteruppsatsen fokuserar på kalkstenars termala egenskaper och mer specifikt om datortomografi (CT) är en bra metod för att särskilja dolomit från kalcit samt om det kan användas för att studera sprickbildning i relation till upphettning. Fyra prov togs från Storugns stenbrott på Gotland och från dessa borrades sex borrkärnor per prov. Därefter undersöktes vilket prov som innehöll mest magnesium genom att analysera proven med syra-test, handhållen XRF och SEM (EDS). Fem kärnor från provet med mest magnesium analyserades därefter med CT-scanning och hettades efter scanningen upp till specifika temperaturer. Temperaturerna som användes var 400, 500, 600, 650, och 700 °C. Efter upphettning scannades kärnorna åter. Programmet Fiji ImageJ användes för att leta upp fem nivåer i bilderna från de obrända proven och därefter lokaliserades samma nivåer i bilderna från de brända proven. Sedan jämfördes bilderna och alla sprickor mättes och markerades. Resultaten visar att CT är en bra metod för att karakterisera sprickor men att mer tid behövs för att modifiera metoden för att då den att fungera för att skilja dolomit från kalcit

Nyckelord: geokemi, kalksten, Gotland, termala egenskaper, XRF, datortomografi

Jessica Jennerheim, Geologiska institutionen Lunds Universitet, Sölvegatan 12, 223 62 Lund, Sweden. E-mail: nat11jje@student.lu.se

Part 1

1 Introduction

In 2011 Vinnova funded a project called *Characterization of physical and chemical properties of carbonate rocks for sustainable and optimized production*. This is a joint project between Nordkalk AB, Kalkproduktion Storugns AB (KPAB) and the Department of Geology at the University of Lund. The goal is to increase the knowledge of the physical and chemical properties of limestone. This study is a part of the project and is divided into two parts. Part one focuses on the geochemistry of limestones, since it's an important factor when it comes to quality. The goal is to determine if XRF scanning is a viable method for distinguishing different types of limestone. Part two uses an X-ray computed tomography (CT) scan to study the effect of thermal heating of limestones.

Limestone can be used in many industrial areas and is commonly quarried as an industrial mineral. One major area where limestone is used is the steel industry, but it is also used in the paper and cement industry, to mention a few. In 2014 there were 16 active limestone quarries in Sweden, four on Gotland, and four dolomite quarries (none on Gotland) (SGU bergverkstatistik 2014). Between 2005 and 2013 an average of 7.8 million ton limestone and 0.5 million ton dolomite were quarried every year, adding up to a total amount of around 8.3 million ton each year. Limestone is also quarried to obtain dimension stone. In Sweden there were 18 active quarries for dimension stone 2014, whereof five of these are located on Gotland. These produced 43 000 ton limestone (SGU bergverkstatistik 2014).

Limestone used by the industry needs to be of high quality when it comes to both chemical and physical aspects (Johansson 2011). Firstly the production is energy consuming, which can raise costs if the material quarried is unusable, and secondly many of the applications do not function if there is, for example, too much contamination. This study focuses on the problems related to the limestone used by the steel industry. The steel industry uses burnt lime and the main problem is that some varieties of limestones tend to break down to finer material, "fines", during calcination. Fines cannot be used by the steel industry. Johansson (2011) looked into why fines form and this will be discussed briefly later on. The goal of this study is to determine whether XRF scanning can be used to see geochemical variation in different types of limestone, if this is connected to the depositional environment, and more importantly if the geochemical variation is an important factor for the steel industry to consider.

2 Background

2.1 Location

In the northern parts of Gotland (Fig 1), close to the village of Bläse, there is a quarry called Storugns (Fig 2). The quarry, run by Nordkalk AB, primarily produces limestone for the steel industry. In order to obtain limestone of good quality, the chemical properties must meet certain prerequisites and levels. As previously stated, Vinnova funded a project in 2011 to increase the knowledge of limestone chemistry and properties. In order to do this a 29.5 m long drill core from the Storugns quarry at Gotland was investigated. The drill core consists of various types of limestone containing sediments that were deposited during the Silurian. The core is part of the Slite Group, which is one of the most widespread lithostratigraphical units of Gotland (Erlström *et al.* 2009). The location of the drill core is just south of the Storugns quarry (Fig 2).

2.2 Depositional environments of carbonates

Carbonate rocks can form in two ways. Either they are formed by precipitation of calcite directly from calcium oversaturated waters or they are made up of allochthonous or autochthonous skeletal carbonate fragments from shell bearing organisms (Flügel 2004). This is a contrast to other sedimentary rocks, where the material mainly derives from erosion, transportation and deposition of detrital material. About 90 % of the modern carbonate rocks have a marine origin (Flügel 2004) but they can also form in non-marine or even terrigenous environments. In shallow marine environments the sedimentation takes place on shelfs (flat) or ramps (inclined), both of which are called carbonate platforms. Carbonate platforms can grow vertically if the sea level rises and laterally when the sea level is stable. If the sea level drops the exposed parts in the top of the platform will usually be eroded (Flügel 2004).

Reefs are one type of carbonate platforms. In reefs the limestone is made up by the animals that lived there and thus their appearance has varied a lot through time. However in general they are made up by massive and very pure limestone (Flügel 2004). The reef itself has three parts (Fig 3); front, core and back (Erlström *et al.* 2009).

The reef core is situated above the normal wave base and therefore contains large structures, usually fossils, such as stromatoporoids, with little matrix between them. The fossils, however, sometimes contain pockets of marl. The reef front is situated between the normal wave-base and storm wave-base and is usually made up by calcirudites. The back of the reef is more protected and tends to be dominated by calcarenite. Neither the front nor the back of the reef contain a lot of matrix but both are mainly made up by debris from the core (Erlström *et al.* 2009).

In front of the reef itself, there is a shallow shelf which is divided into a distal and proximal part. The proximal parts contain material that have been swept out on the shelf and can vary between calcarenite and calcilutite. The more distal parts are made up of marl/marlstone and sometimes calcilutite. In the marl/marlstone of the shallow shelf, the carbonate and siliciclastic minerals make up equal parts and there are usually alternating bedding sequences of marl/ marlstone and calcilutite.

Behind the reef there are usually lagoonal areas. Here the distal parts consist of marl/marlstone and calcilutite, just like the shallow shelf. The proximal parts consist of calcilutite, calcarenite or algae limestone that contain few fossils.

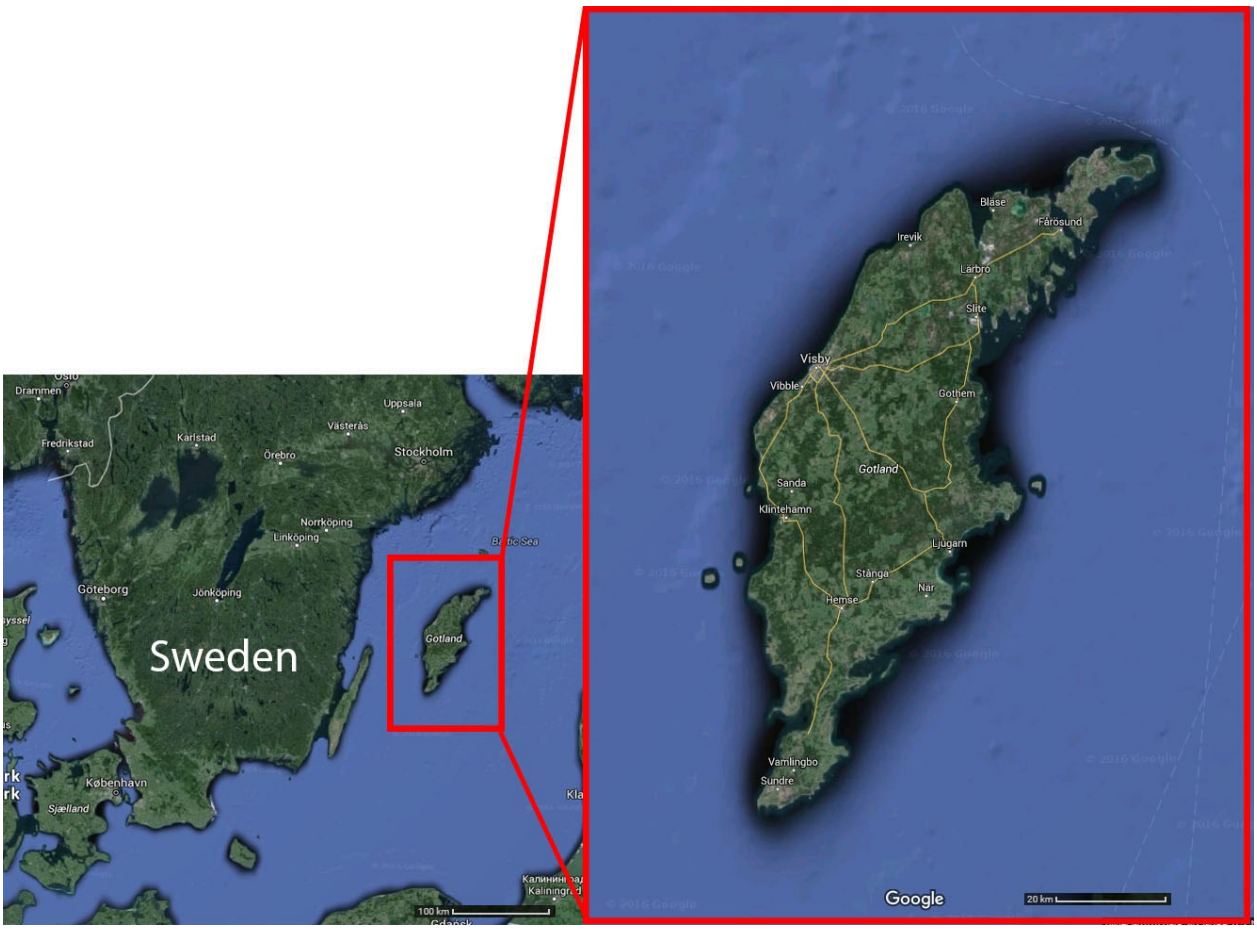

Fig. 1. Shows the location of Gotland. The framed area on Gotland in shown in figure 2. Source: modified from Google maps 2016.

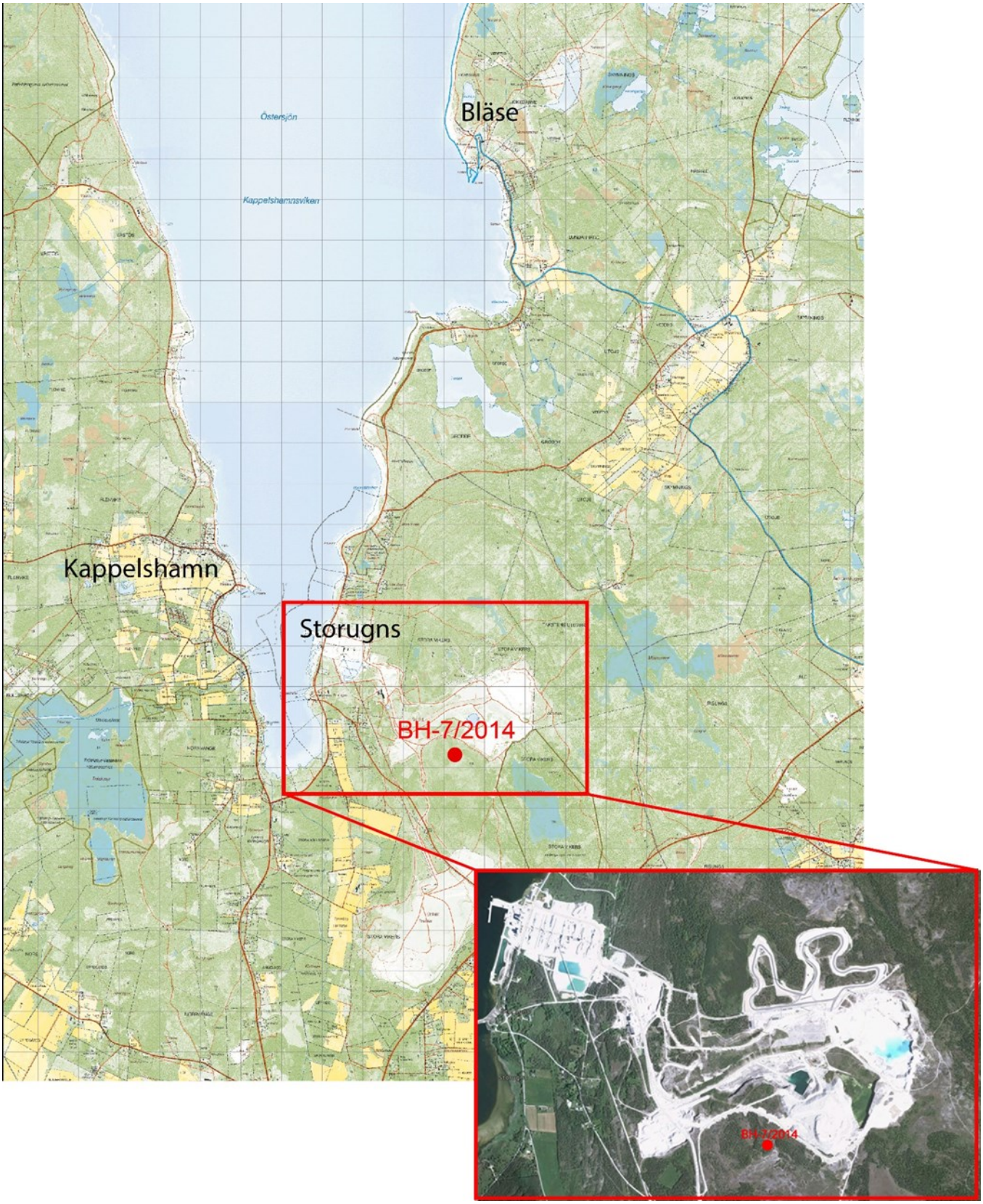

Fig. 2. Shows a map of northern Gotland where the position of the drill core is marked in red. Coordinates (RT90 2.5 gonV 0:-15 System); X: 6415657.1, Y: 1679622.7, Z: 37.8. Source: Nordkalk AB, modified from Lantmäteriet 2016 and Google maps 2016.

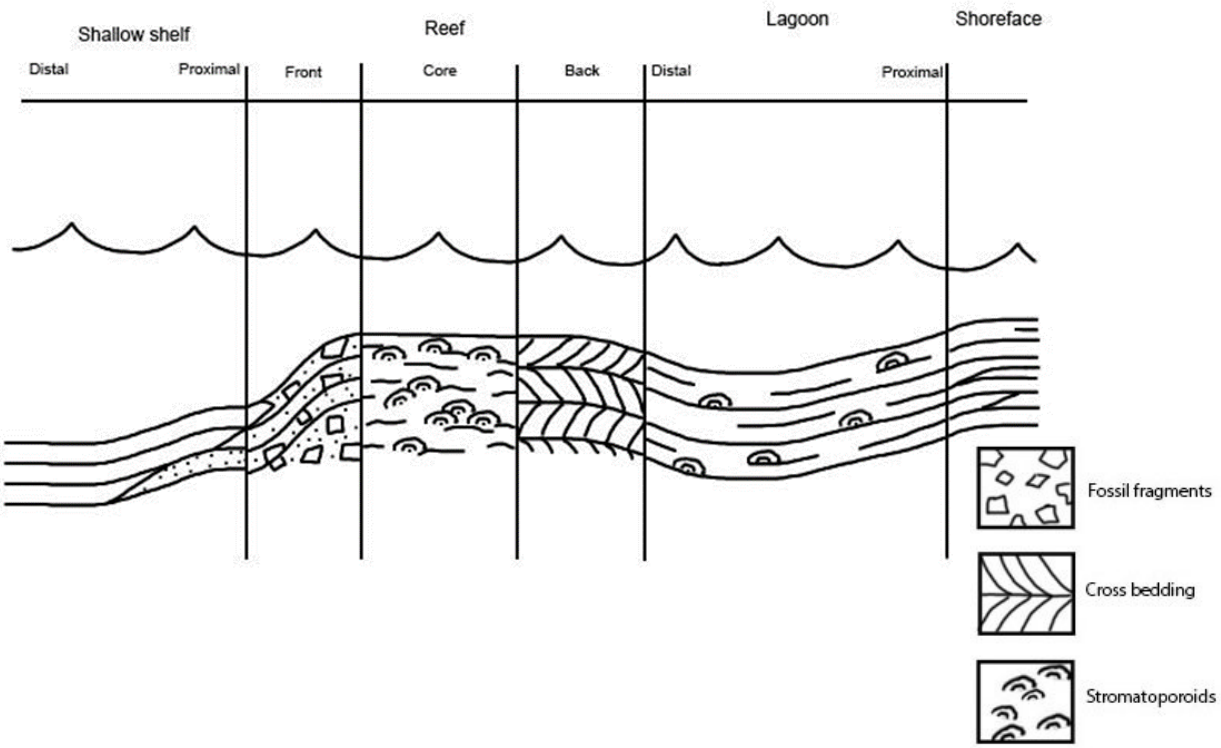

Fig. 3. Schematic picture of the different parts of a reef. Modified from Erlström *et al*. 2009.

2.3 Chemical properties of limestones

Carbonate rocks are overall dominated by a high amount of calcite ($CaCO_3$) or its polymorph, aragonite. Usually the calcite content is shown as calcium oxide (CaO), and calcarenites and calcirudites show the highest amounts (52-55 %). Reef limestone and stromatoporoid limestone also show high values of CaO but the amounts are generally lowered due to the fact that these rocks also contain small amounts of marl/marlstone. The marl/marlstone also results in higher amounts of for example SiO_2, K_2O and Al_2O_3, which are related to the mineralogy of the occurring clay minerals. In limestone SiO_2 values are usually low (<2 %) but if the rock contains a lot of clay minerals these values will rise, in rare cases up to as much as 30-40 %. K_2O and Al_2O_3 usually follow the variations in the SiO_2 levels since these components are also related to the amount of clay minerals in the rock (Erlström *et al*. 2009).

Another important mineral is dolomite ($Ca,Mg(CO_3)_2$), which is relatively common in marl/ marlstone and calcilutite, especially in rocks of the Slite Group (see below). Apart from carbonates there are small amounts of pyrite (FeS_2), especially in more clay mineral rich sediments or in fractures in reef limestone. Iron, expressed as Fe_2O_3, is also most commonly found in clay mineral rich rocks, such as marl, where it can reach 1-3 %, compared to <0.5 % in other carbonate rocks. The carbonates of Gotland contain quite large amounts of strontium, 100-300 ppm, whereas most other trace elements are below 10 ppm. For example uranium can reach around 2-8 ppm locally (Erlström *et al*. 2009).

2.4 The sedimentary bedrock of Gotland

Sedimentary bedrock can be found everywhere on Gotland. The sedimentary bedrock range from the Cambrian to the Silurian but the Cambrian and Ordovician depositions can only be seen in deep drill cores (Erlström *et al.* 2009). The Silurian bedrock (Fig 4) of Wenlock and Ludlow is around 428-418 Ma, and contains a 500-750 m thick succession of strata. The deeper parts of the strata are dominated by argillaceous limestones, marl and mudstone whereas the shallower parts contain different types of limestone, such as stromatoporoid limestone and reef limestone. Not only is there a difference in the rocks between deeper and shallower depositions, there's also a difference laterally. Generally the bedrock is dominated by more carbonate rich rocks (Erlström *et al.* 2009), such a limestones (Manten 1971), in the north and muddier rocks (Erlström *et al.* 2009), such as marlstone (Manten 1971) in the south. Most of the rocks were deposited in cycles, with periods of erosion, on a shallow marine shelf (Erlström *et al.* 2009).

This study focuses on a drill core from the Silurian Slite Group, which was deposited during the Wenlock. The Slite Group is geographically the most widespread litostratigraphical unit in the north of Gotland. The group is thick, approximately 100 m , and is composed of a series of different carbonate rock types that were described and stratigraphically divided into 7 units (a-g) by Hede (1960). Calner (1999), described one additional group, summing up to 8 units. There are five major types of bedrock in the Slite Group used by SGU in their map description K 221; marl and marlstone, calcilutite, calcarenite, calcirudite and different kind of reef limestones. Each of these rock types will be described in the following part. This classification

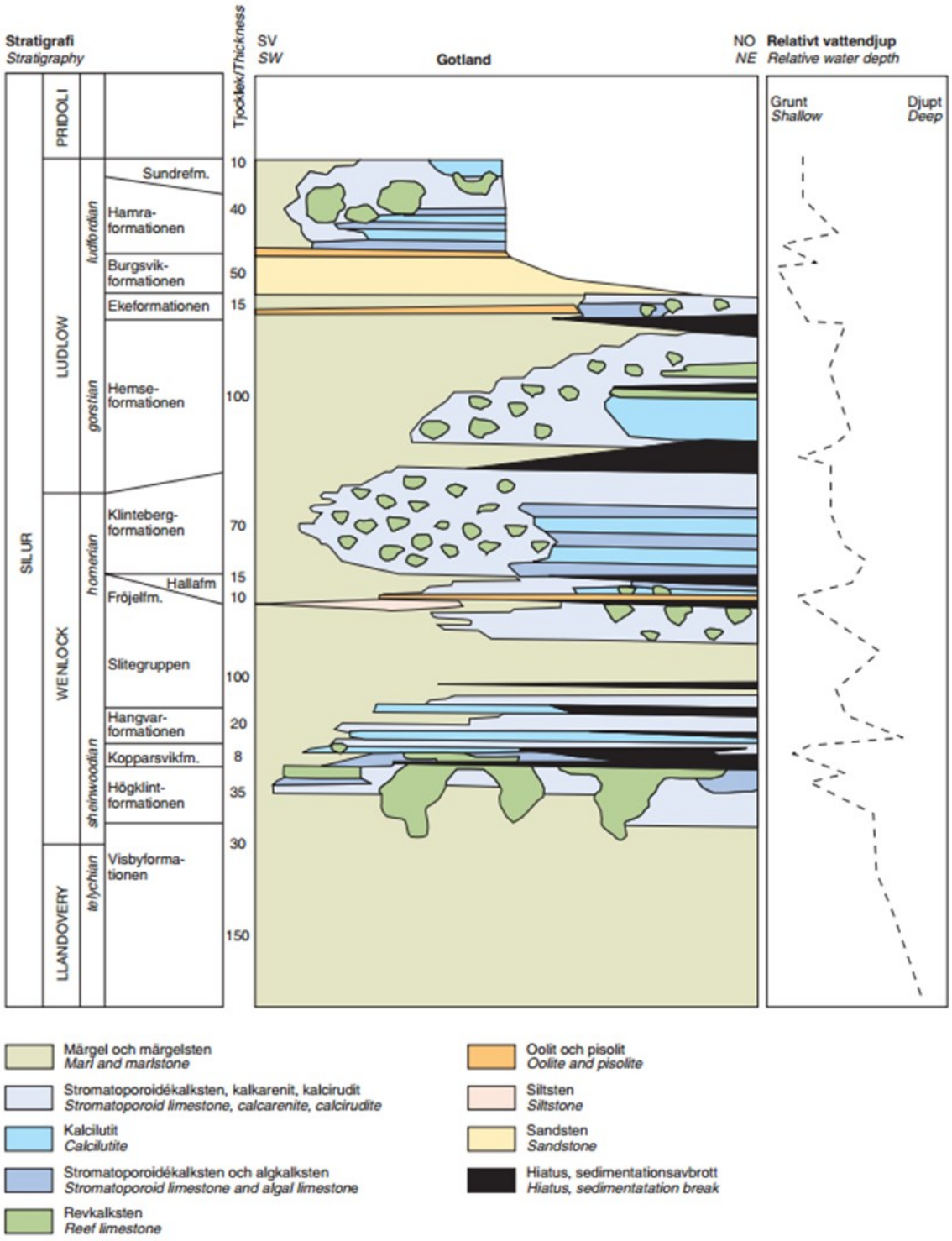

Fig. 4. Schematic log of the Silurian bedrock on Gotland. Source: Erlström *et al.* 2009.

will be used in this study and is described below.

Marl and marlstone: The difference between marl and marlstone is that marlstone is solid while marl is poorly consolidated. Marl and marlstones represent deposition in the distal parts of the shelf or in distal lagoons behind the reefs, where the water energy is generally low. They are very common rock types on Gotland and are usually layered with intervals of soft to hard marl and hard, crystalline limestone, such as calcilutite. The individual layers are usually thin, around 10 cm, and the marls themselves are seldom thicker than a few cm. Marlstone usually contains smaller fossil fragments and is grey-blue to dark-grey in colour.

Calcilutite: Calcilutite is a fine grained and very dense limestone, where the individual grains cannot be seen by the naked eye. The rock type usually contains a lot of matrix consisting of clay and micrite. Calcilutite usually have a dull beige to grey colour and contains more carbonates than clay minerals. Sometimes this rock type occurs together with marl or marlstone and is deposited in distal to proximal shallow shelfs or in lagoons.

Calcarenite: Calcarenite contains rounded carbonate grains in the sand fraction (0.063-2 mm) and can sometimes show a clear lamination. The rock type is often well sorted and with a distinct crystallinity. Calcarenite contains a high amount of sparite cement, which fills up pore space, but contains little to no matrix. Just like calcilutite and marlstone, calcarenite is related to shallow shelfs or lagoonal depositional settings. However this rock type reflects depositional setting on the proximal parts of the shelfs as well as lagoons. The original deposition of the included sediments could also have been in the back parts of the reef itself, sometimes together with stromatoporoids.

Calcirudite: Contains crystals >2 mm and usually large fossils, such as crinoids. Since it is not very well cemented, this rock type is porous and breaks easily. Usually this rock type doesn't contain any matrix due to the fact that it is formed in the reef front, where the water energy is too high to deposit any fine grains.

Stromatoporoid limestone: The main criterion for this rock type is that stromatoporoids dominate the rock, yet don't grow intertwined. Since stromatoporoids have many different shapes and sizes, these rocks can vary in appearance. A matrix of calcilutite or calcarenite is common between the stromatoporoids. The stromatoporoids themselves are usually finely crystalline, dense and thinly laminated. Although the colour varies, a dull beige or nougat brown colour dominate and sometimes they also contain small inclusions with greenish marl. These rocks usually represent the core of the reef but differ from the reef limestone due to the fact that the stromatoporoids are separate although numerous, whereas in reef limestone they grow tightly together (personal communication, Mikael Erlström, 20 November 2015).

Reef limestone: The reefs are formed by different fossils but mainly stromatoporoids, crinoids, corals, algae and bryozoans. There is no clear layering, instead the fossils making up the reef are intertwined in chaotic patterns. The matrix between the fossils usually consists of light green marl but calcite filled cavities are common. Minor pyrite mineralisations are also frequent. Reef limestones represent the reef cores.

Fragment reef limestone: This is a rock type found in the drill core consisting of fragmented parts from the reef core with a fine-grained coating of algae around. The fragments are usually only a few cm and the coating of algae varies from grey to light green.

2.4.1 Chemical properties of the Slite Group

Shaikh *et al*. (1990) presented chemical data on limestone sampled at various locations on Gotland (Appendix 1). These results can be seen as a reference on the general geochemistry of the limestone and marl from the Slite Group. The data is based on 60 m drill cores from different parts of the Slite Group. An average as well as the minimum and maximum values of CaO, SiO_2, Al_2O_3, TiO_2, Fe_2O_3, MnO, MgO, K_2O, Na_2O and S is summarised in table 1. The data is based on the results presented in Shaikh *et al.* (1990) for the limestone and marl of the Slite Group. The results show that CaO is usually around 53 % in limestones and 40 % in marls. The SiO_2 is higher in marl but varies a lot depending on how rich in clay minerals the marl is. Al_2O_3 follows the SiO_2 curve, but generally only reaches a few percent.

2.4.2 Chemical properties of the Storugns limestone

Shaikh *et al*. (1990) also collected data from Storugns. Table 2 shows the average results of the same elements as in table 1, above. In addition to the main chemical components Shaikh *et al*. (1990) also present data regarding trace elements and this is shown in table 3. Overall Storugns has a very high CaO content (about 53 %) and low SiO_2 and Al_2O_3 (around 1.55 % and 0.76 % respectively). The magnesium levels are also relatively low (around 0.8 %) which is related to a low amount of dolomite and that the calcite is mostly low-mg calcite (Shaikh *et al*. 1990).There are also small amounts of iron (about 0.3 %) as well as a minor contribution of potassium. Trace elements show overall low concentration, usually below detection limit, but there are some exceptions, such as barium, that varies between around 2-28 ppm, and strontium, that can reach levels around 180 ppm (Shaikh *et al.* 1990).

2.5 The formation of fines

Fine material formed during calcination of limestones (fines) cannot be used by the steel industry and limestone prone to yield higher amount of fines are therefore regarded as unusable. In 2011, Johansson looked into the formation of fines and discovered that their appearance isn't connected to one simple factor but rather many connected factors. Firstly Johansson (2011) states that one important factor is the presence of calcite-healed fractures in the limestone. Increased amounts of fractures tend to produce more fines when heated during calcination. Secondly another important factor is the texture of the limestone. A well crystallised calcite structure and larger grain size both contribute to the formation of fines. Mineral inclusions, stylolites (serrated surfaces created by pressure) and liquid inclusions don't affect the formation of fines but can still be problematic as they may affect the mechan-

Table 1. The table shows the average, minimum and maximum of the major elements in (weight percent) of the limestone and marl of the Slite Group. Shaikh *et al. (*1990). *values below detection limit

Limestone	Average Weight %	Max Weight %	Min Weight %
CaO	53.14	55	49.5
SiO_2	1.89	5.4	0.4
Al_2O_3	0.73	1.32	0.29
TiO_2	0.03	0.07	0*
Fe_2O_3	0.36	0.72	0.17
MnO	0.02	0.03	0.01
MgO	0.70	1.22	0.18
K_2O	0.20	0.48	0.04
Na_2O	0.04	0.06	0.02
S	0.02	0.12	0*
Marl	**Average Weight %**	**Max Weight %**	**Min Weight %**
CaO	41.57	49.6	33.5
SiO_2	13.00	20.7	5.7
Al_2O_3	2.69	4.21	1.17
TiO_2	0.15	0.24	0.05
Fe_2O_3	1.13	1.42	0.68
MnO	0.07	0.13	0.04
MgO	2.87	4.93	0.19
K_2O	0.89	1.51	0.38
Na_2O	0.17	0.21	0.1
S	0.14	0.21	0.04

ical properties of the rock. For example they may be problematic during crushing. This complexity leads to the conclusion that each type of limestone must be evaluated separately regarding its ability to produce fines during the heating and calcination process (Johansson 2011).

3 Methods

3.1 Core logging and cutting

First the drill core's lithological characteristics was described using the classification of rock types presented by SGU in their map description K221 (Erlström *et al.* 2009, see above). A log was drawn with a corresponding rock description for each layer.

Based on the lithological description and identification of different layers five core samples representing different limestone types were selected and split with a rock saw. The samples were taken at 6.28-6.32, 11.00-11.18, 18.10-18.25, 24.60-24.81 and 29.17-29.36 meters. The sawed samples were polished and scanned in high resolution with a photo scanner. Note that there is one split for each rock type except for the marl since it was too soft to cut successfully.

3.2 XRF

Table 2. Shows the average chemical data of two drill cores from Storugns quarry. Source: Shaikh *et al.* (1990)

Storugn - Chemical data	Weight %
CaO	53.3
SiO_2	1.55
Al_2O_3	0.76
TiO_2	0.03
Fe_2O_3	0.34
MnO	0.02
MgO	0.81
K_2O	0.21
Na2O	0.3
S	0.08

Table 3. Shows the average chemical data of the trace elements in Storugns. Source: Shaikh *et al.* (1990)

Storugn - Trace elements	ppm
Ba	1.9-28.7
Co	0.6
Cr	1-3
Cu	3-4
Sr	170-188
Zn	5.6-30.4
V	2-3

XRF (x-ray fluorescence) is a quick method to determine the composition of both liquids and various kinds of solids. Not only is it a fast and high precision method but it also requires minimal sample preparation, making it highly useful. XRF is based on x-rays that are emitted from an x-ray tube and as they hit the sample, the atoms in it get excited and emit fluorescent x-ray radiation. This radiation is emitted as photons with a specific energy for each element. A detector will then read the energy spectra and determine not only which elements (qualitative measurement) are present but also how much (quantitative measurement) there is of each element. Sometimes a filter is used to increase the overall quality of the XRF by improving the signal to noise ratio. The result is an energy spectra where the peaks represent the elements present whereas the peak-area is proportional to the amount of each element. This peak-area can be transformed into weight percent (Bruower 2010).

In this study the entire drill core was scanned with a high resolution XRF scanner (ITRAX), developed by Cox Analytical. This was done in Malå by AlS Minerals. The high resolution ITRAX equipment scans a narrow trace along the drill core and measures the average chemical composition at each cm in weight percent.

3.3 Handheld XRF

A handheld XRF was used to analyse the five split parts of the core. 20 spots were chosen randomly for analysis on each rock type except for the reef limestone. Here only 10 points were chosen due to the fact that the piece was too small as to enable additional analysis points. The data was transferred to excel and the average amount of each element was calculated in weight percent. However no diagrams were created with the data since the depth of the test points wasn't an important factor. The method was applied as to validate and compare the results from the ITRAX scanner and the hand held instrument.

3.4 Computer analysis

The results from the ITRAX scan were analysed with two different computer programs. First a program called Tray-sum was used. In Tray-sum the peak area for different elements can be placed as an overlay on top of a picture of the drill core. This provides the user with a visualisation of the relative variations in abundance and location of anomalies in the core. However, it was hard to connect the chemical data specific levels of the core since there was no depth correlation between the two. Therefore the focus ended up on Q-spec.

The Q-spec program shows the chemical composition of each meter of the drill core as weight percent per cm. The program can also create excel files and will create one file per meter unless a specific interval is chosen. Each excel file will then include all elements that were analysed. These excel files with quantitative data were used for the rest of this study.

In Excel, diagrams were made using the files created by Q-spec. Each element of interest was plotted against depth. This makes anomalies easy to see and locate since they will appear as positive or negative anomalies. The tables were also used to see overall values from different parts of the core and these were used to attempt to identify the different rock types. After the rock types were interpreted, averages and ranges of CaO and SiO_2 for each rock type were calculated and compared. The remaining major elements as well as trace elements were evaluated for differences as well.

3.5 Students t-test

The student's t-test is used to determine whether there is a significant difference between two test groups (for instance calcarenite and marl) with normal distributions by comparing the means of both groups (Haynes 2013). Simplified, the student's t-test compares the curves for both of the groups and determines the overlap to see whether they are similar or not. In order to conduct a student's t-test a null hypothesis is created, usually that there is no difference between the groups. If the null hypothesis can be rejected there is a statistically significant difference.

The result of the t-test will appear as a p-value (Encyclopedia of Public Health 2008). If this value is below an already set level (usually 0.05) the null hypothesis can be discarded. However it's important to remember that a smaller p-value doesn't necessarily mean a greater effect as the p-value is also related to how easy it is to detect an association. This makes the experimental design very important to the final result.

3.6 SEM

In order to confirm what minerals beside calcite and dolomite are present in the core, one sample from each rock type was dissolved in acetic acid. This was done on the already split parts of the core, thus excluding the marl. When all the calcite had been dissolved the samples were dried and put onto coal fibre tape. The samples were then analysed with a scanning electron microscope (SEM). SEM uses an electron source, called electron gun to accelerate electrons and focus them into a beam which hits the sample. The collision with the sample will produce two types of electrons; secondary and backscatter. The secondary electrons create light when they hit the scintillator material and the light will be transformed into an electric signal. The variation in this signal is then measured by a detector. The backscattered electrons are measured by another detector. To get the best possible picture the electron beam should be wide and the current stable (Goldstein *et al.* 1992).

In order to get a qualitative estimation of what minerals beside calcium and dolomite are present in the core an x-ray spectrometer can be used. There are two kinds of x-ray spectrometers; energy dispersive spectrometer (EDS) and wavelength dispersive spectrometer (WDS) (Reed 2005). In this study an EDS was used. EDS records all x-ray energies simultaneously using a semiconductor made of germanium or silicone. When the x-ray photons are absorbed by the detection medium, auger and photo electrons are generated. These create a current pulse that is proportional to the photon energy. This pulse is then amplified and converted to a spectrum that can be displayed as a histogram. These can be both logarithmical and linear and usually display counts per channel against energy (keV) (Reed 2005).

4 Results

4.1 Logging

The lithological description of the core showed that almost half of the core, 14 m, consists of calcarenite (Fig 5). There are also moderate amounts of stromatoporoid limestone, around 6 m, and calcilutite, around 4 m. The calcilutite sometimes contain fine layers of marl. There are also some minor intervals that are dominated by marl, around 1 m, in the lower portion of the core. Two intervals of the core is composed of reef limestone and fragment limestone respectively. These intervals are almost exclusively composed of stromatoporoids although the fragment limestone also contains bryozoans, crinoids and other undistinguishable small fossil fragments. Many of the calcarenite layers also contain various amounts of stromatoporoids, usually around 5 cm in size. Table 4 shows the colour and presence of stylolites in each layer as well as a short description. For a full description of each layer see appendix 2.

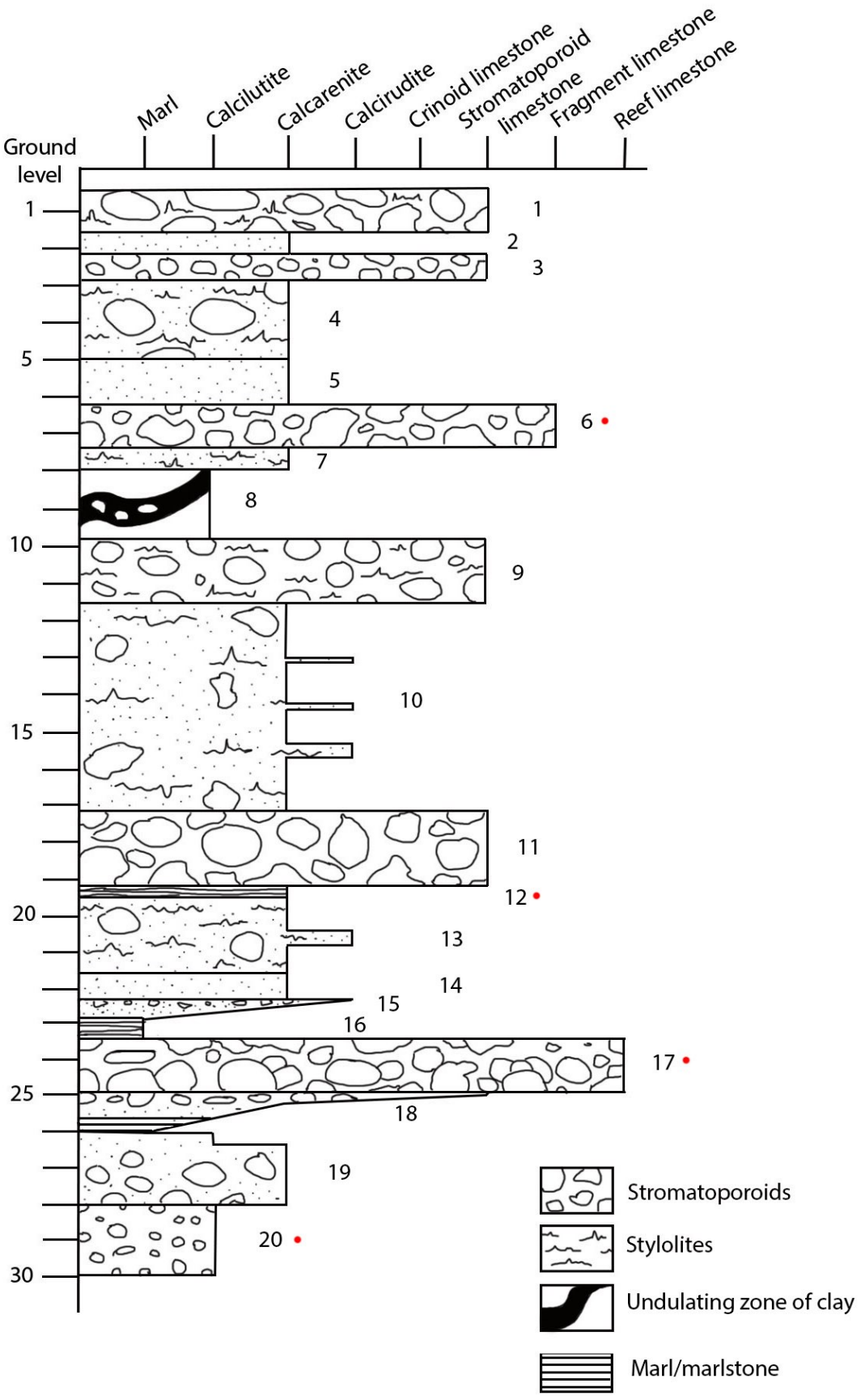

Fig 5. A log of the entire drill core. The numbers correspond to the layers presented in table 4. The red dots show the layers from which samples representing each type were collected.

Table 4. Shows the presence of stylolites (serrated surfaces created by pressure) in each layer of the co re as well as a short description.

Layer	Rock type	Colour	Stylolites	Description
1	Stromatoporoid lime-stone	beige	x	Pink stromatoporoids (5-10 cm) with a calcare-nitic matrix
2	Calcarenite	grey	x	Calcarenite with a argillaceous matrix
3	Stromatoporoid lime-stone	grey	x	Pink stromatoporoids (3-10cm) with a calcare-nitic matrix. Calcite filled fractures.
4	Calcarenite	grey	x	Crystalline with red crinoid fragments and oth-er white fossil fragments. Calcite filled frac-tures
5	Calcarenite	dark grey	x	Crystalline with fossil fragments
6	Fragment limestone	grey/blue to green	x	Fragments of fossils such as stromatoporoids, bryozoans and crinoids with a greenish, micrite matrix.
7	Calcarenite	beige	x	Contains small fossils
8	Calcilutite	dark grey	x	No sharp boundaries to adjacent layers. Con-tains “flowy layers” that are dark, argillaceous and filled with small fossil fragments.
9	Stromatoporoid lime-stone	beige	x	The stromatoporoids have un-sharp bounda-ries. Contains many stylolites of various sizes.
10	Calcarenite	grey	x	Contains abundant crinoids and other fossil fragments. Some layers are calcirudite. Sharp lower boundary.
11	Stromatoporoid lime-stone	beige	x	Reef-like in places. Calcarenitic matrix.
12	Calcarenite	beige	x	Clear lamination
13	Calcarenite	grey	x	Crystalline with abundant stylolites. Layers of calcirudite
14	Calcarenite	dark grey	x	Small pyrites mineralisations in fractures
15	Calcirudite to calcarenite to calcilutite	grey	x	The calcarenite gradually grades into calcilut-ite.
16	Marlstone with layers of calcilutite	dark to light grey		Thin layers of marl (10 cm) with an interlayer of calcilutite
17	Reef limestone	grey to dark grey		Dominated by stromatoporoids. Pockets of marl within stromatoporoids. Scattered layers dominated by crinoids.
18	Calcarenite to calcilutite/ marl	grey to dark grey	x	The lower part varies between marl and calci-lutite
19	Calcilutite	beige		Contains fossil fragments
20	Calcilutite	beige	x	Abundant fossils

4.2 ITRAX - Geochemistry

As stated before the data was measured differently than previous studies, making these values impossible to correlate with others from the Storugn area. This data will therefore only be used to compare the rock types within the core. The elements/components which were analysed were; Al_2O_3, SiO_2, P_2O_5, S, Cl, Ar, K_2O, CaO, TiO_2, V, Cr, MnO, Fe_2O_3, Ni, Cu, Zn, Ge, Rb, Sr, Y, Zr, Cd, In, Ba, Sm and Eu. Out of these elements, focus was put on silica and calcium oxide as they are the most abundant elements in the core.

4.2.1 Major elements

The more common elements in the core, besides calcium, such as silica, iron and potassium (Fig 6) follow each other very well. This is also true for aluminium (Fig 7), although it is not as obvious as with the iron and potassium relationship. The iron (measured as Fe_2O_3) levels are usually stable around 0.3 % but can sometimes reach as high as 1-2 % in some parts of the core. These peaks follow the same pattern and trend as the silica curve. The same is noted for potassium (K_2O), which varies from 0.01 % up to almost one percent. The amount of aluminium (Al_2O_3) varies significantly more than potassium or iron, appearing more like the silica curve, although the peaks are not always correlated with each other. Both the silica and aluminium values are usually around 4 % in the limestone while reaching as high as 12 % in the marl.

The rest of the major elements don’t follow the silica curve but seem to occur sporadically. For instance small amounts of sulphur (S) exist locally in some parts of the core with areas devoid of sulphur in

between. The amount of sulphur reaches values between 0.1 and 0.5 %, which is slightly higher than in previous studies, done by Shaikh *et al.* 1990 (all references to previous studies are here forth referring to Shaik *et al.* 1990). The occurrence of sulphur does not seem related to any other specific element or rock type. The titanium content is also slightly higher than in previous studies and the amount is generally higher in the calcarenite, stromatoporoid and reef limestones, where it reaches around 0.06 %, in comparison with slightly less amounts (around 0.04 %) for the other rock types. The manganese content varies between 0.01 and 0.02 % and the magnesium between 0.02 and 1.1 %. The magnesium content, however, is associated by significant errors (very high error bars) and the data should therefore only be seen as an indicator whether magnesium is present or not. This is because light elements are difficult to measure using XRF (personal communication M. Erlström june 2016). Most peaks of magnesium are found in the fragment limestone, where the average is 1.1 %.

One element that does not follow the silica curve, but rather does the opposite is calcium (Fig 8). The amount of calcium (CaO) measured by the ITRAX scanner is lower than expected in the entire core. Generally the CaO content varies between 40-42 % for the limestone layers and 35 % for the marl layers.

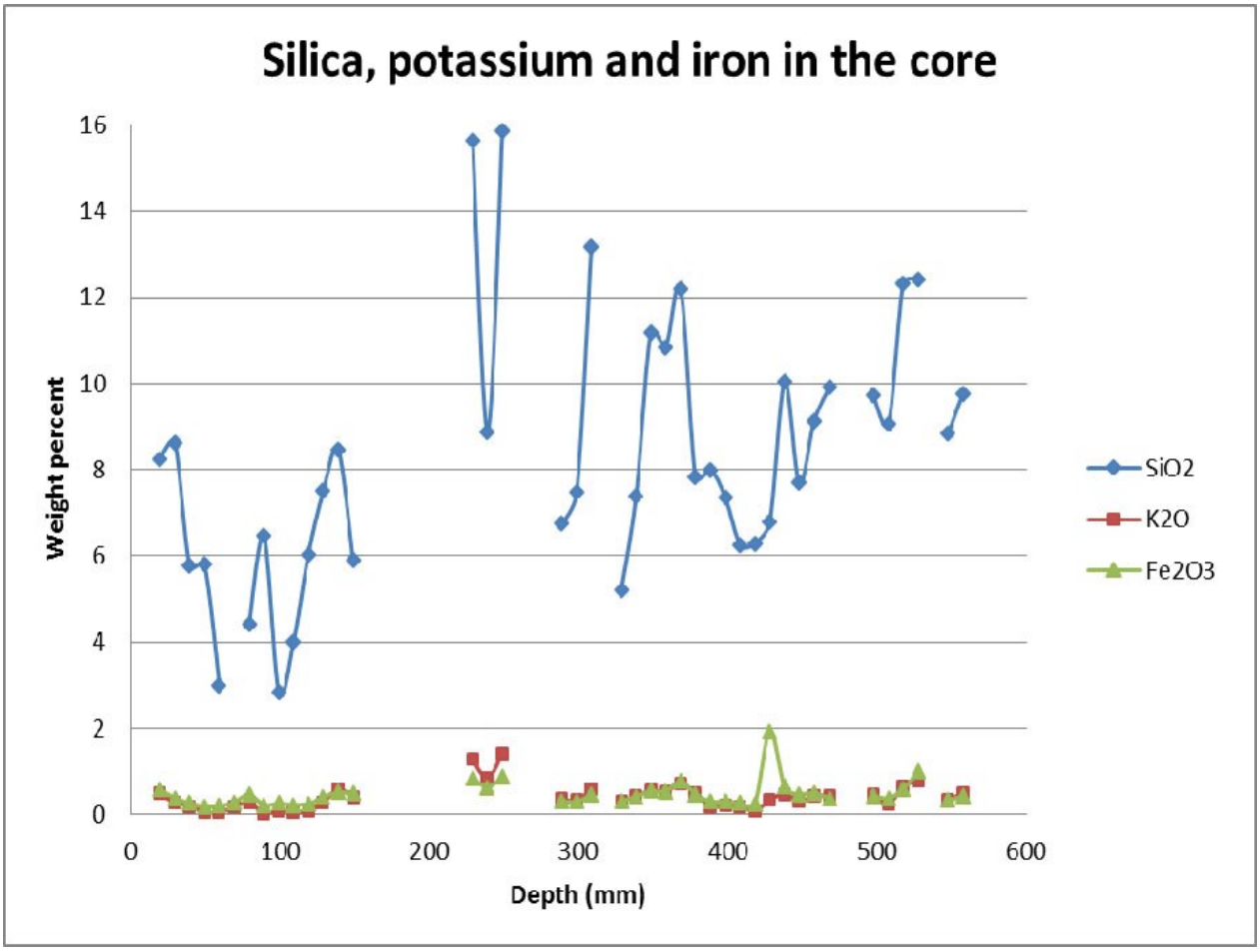

Fig 6. Shows the content of silica, iron and potassium in 60 cm of the core (about 6 m down). Note that the parts that couldn't be scanned by the ITRAX show up as gaps in the diagram.

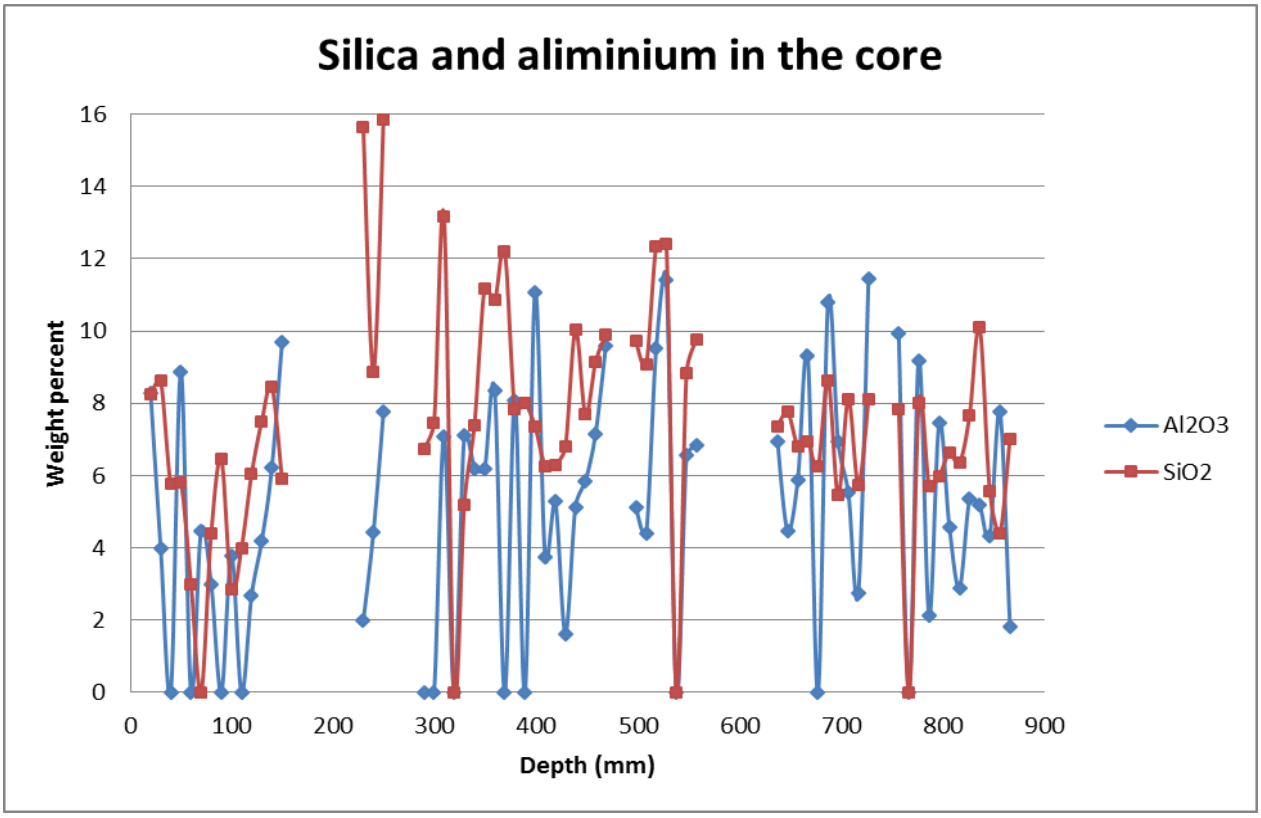

Fig 7. Shows the aluminium and silica content of 90 cm of the core (about 6 m down). Note that the parts that couldn't be scanned by the ITRAX show up as gaps in the diagram.

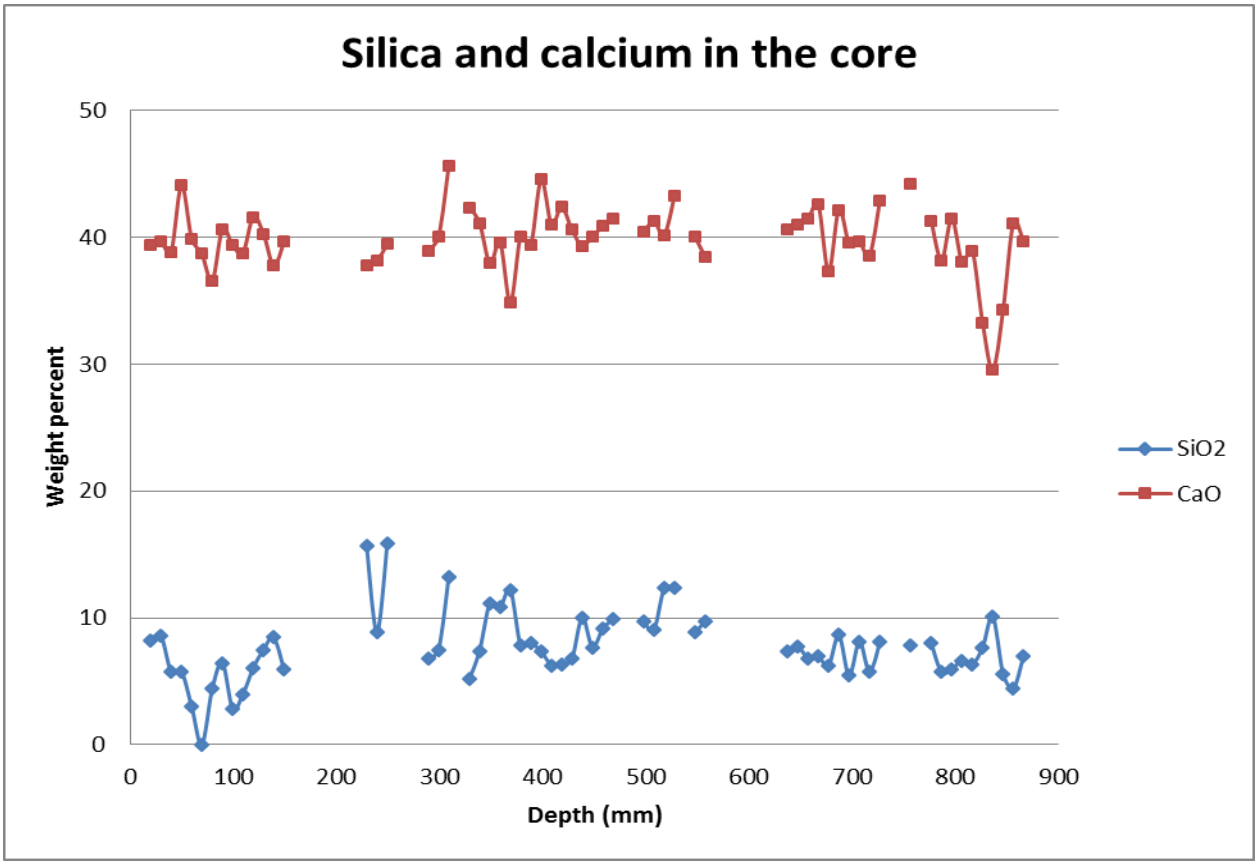

Fig 8. Shows the amount of calcium and silica in 90 cm of the core (about 6 m down). Note that the parts that couldn't be scanned by the ITRAX show up as gaps in the diagram. Also note that silica is represented by blue points in this figure and red in the previous figure.

4.2.2 Trace elements

Many of the trace elements in the core show higher concentrations than previous studies. They mostly appear as scattered peaks, although the amount varies. For example, this is true for barium, which has an average of about 200 ppm in the peaks of the core, compared to the 1.9-28.7 ppm in previous studies. Much like the other minor elements, barium appears sporadically throughout the core, with a few anomalies. The amount of chromium is also high in comparison to previous studies, around 10-100 ppm. In fact the amount is rarely under 10 ppm but since there are many intervals without any chromium the average for the entire core is only 4 ppm, which is close to the amount specified in the previous studies. The copper behaves in a similar way to chromium, with the high peaks around 10-20 ppm and a normal average (compared to previous studies) if the whole core is compared and this is also true for the barium. In previous studies the vanadium amount is around 2-3 ppm but in the investigated core it reaches 20-30 ppm in all rock types except in the fragment limestone, where the concentration is as high as 100-300 ppm. The zinc level is also higher (37-368 ppm) compared to previous studies (5.6-30.4 ppm). The strontium level is the only minor element which gives lower values from the ITRAX scanning in comparison to previous studies (75-122 ppm compared to 170-188 ppm).

The occurrence of trace elements does not show any correlation with rock type. For instance, the small peaks of barium cannot be related to a specific rock type or any other element. Most of the trace element concentrations show a wide range of values in comparison with previous studies. One example is the amount of strontium which ranges between 145 and 200 ppm in the studied core in compassion to a range between 170 and 188 ppm in older data from Storugns.

4.3 Geochemistry of the rock types

4.3.1 Marl /marlstone

Marl/marlstone dominated parts are only present in two minor intervals of the core, both of which are located in the lower parts. The intervals consist of an alternating sequence of grey-greenish to grey marlstone and light grey to grey calcilutite. The layers are 10 cm thick, undulating and intertwined with each other, which makes the interval a characteristic heterogeneous bedding sequence. The marl/marlstone contains high amounts of SiO_2 (on average 12 %), and low amounts of CaO, around 35 % (table 5). This is the highest respectively lowest values compared to all other rock types in the core. Although the range of values for both elements is quite big, the amounts do not appear to fluctuate a considerable deal. The range derives from a few interbeds and lenses with calcareous clay (not marl) which significantly affects the values for the CaO and SiO_2 (Fig 9).

Table 5. Summary of the average, range and standard deviation (in weight percent) of SiO_2 and CaO in marl.

	SiO_2 Weight %	**CaO Weight %**
Average	12.1	35.34
Range	7.2-25.6	19.7-42.0
Standard deviation	4.12	4.0

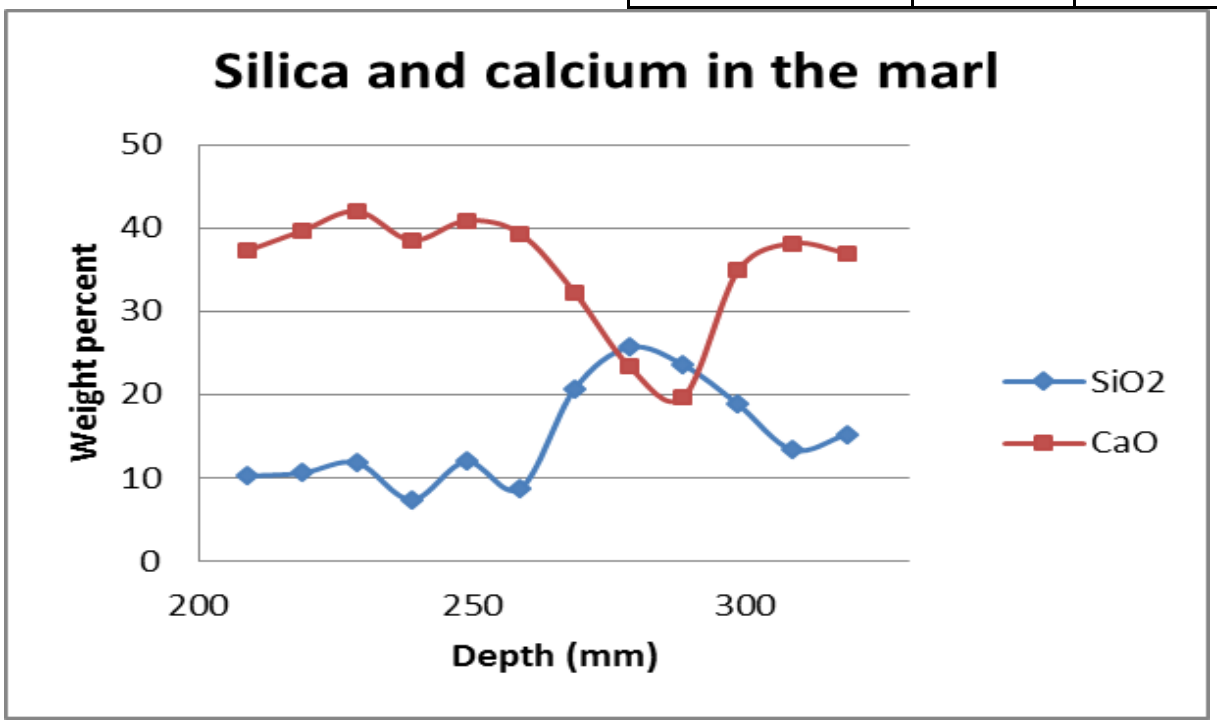

Fig 9. Shows the amount of silica and calcium in ca 35 cm of the core (about 26 m down). The relative high SiO_2 and low CaO corresponds to a lens of calcareous clay.

4.3.2 Calcilutite

Beside the calcilutite in the marl/marlstone interval, calcilutite occurs frequently in other parts of the core, often mixed and with fossil fragments. Two intervals dominate and make up approximately four meters of the core.

The typical calcilutite is light beige to slightly grey and contains smaller fossil fragments (Fig 10) of varying abundance. In some places the abundance is so high the calcilutite could be classified as a fragment limestone with a micrite matrix. Entirely pure calcilutite isn't present in the core.

The calcilutite generally displays relatively narrow ranges of values for most elements (Fig 11) with a CaO content of about 41 % (table 6). The SiO_2 value is just below 4 %, which is the lowest SiO_2 average out of all the investigated rock types. The only exception of these low SiO_2 values seems to be where clay rich stylolite seams are present and in some generally more argillaceous areas of the drill core. The calcilutite displays the narrowest SiO_2 range out of all the rock types. It varies between 0-11 % compared to fragment limestone and calcarenite which varies between 0-20 % (see below).

Table 6. Shows the average, range and standard deviation (in weight percent) of SiO_2 and CaO in calcilutite.

	SiO_2 Weight %	**CaO Weight %**
Average	3.75	41.26
Range	0-10.65	25.5-47.0
Standard deviation	3.54	4.0

Fig 10. A sample of calcilutite from the core (about 28 m down).

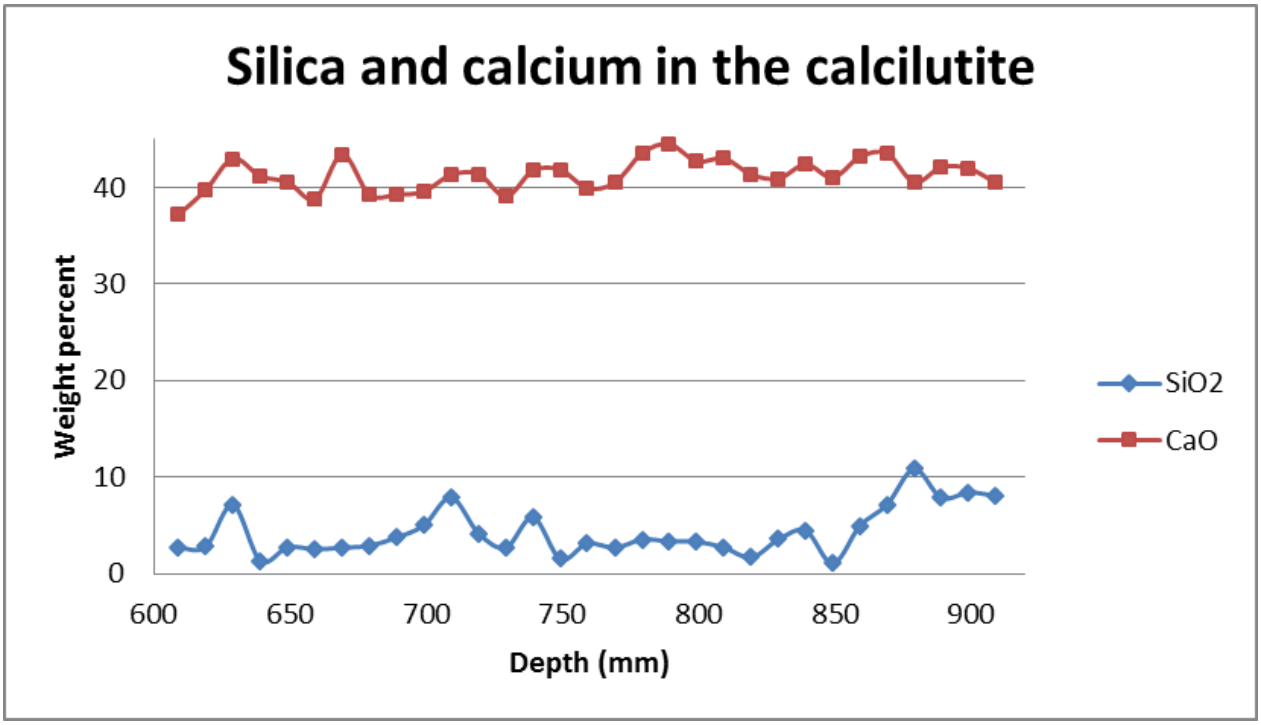

Fig 11. Shows the amount of silica and calcium in 30 cm calcilutite (about 26 m down).

4.3.3 Calcarenite

The calcarenite varies in appearance throughout the core. For example there are some parts that are clearly crystalline and others that aren't. However crystallinity is generally visible and in some cases layering (Fig 12) can be seen as well.

The calcarenite show relatively stable values of SiO_2, around 5 %, and CaO, around 40 % (table 7), which are intermediate levels in comparison to the other rock types. In general the SiO_2 varies more than the CaO values, which are fairly uniform (Fig 13).

Table 7. Shows the average, range and standard deviation (in weight percent) of SiO_2 and CaO in calcarenite.

	SiO_2 Weight %	**CaO Weight %**
Average	4.9	40.21
Range	0-20.31	20.53-46.91
Standard deviation	2.63	3.89

Fig 12. A sample of calcarenite from the Core (about 19 m down). Note the clear lamination and stylolites.

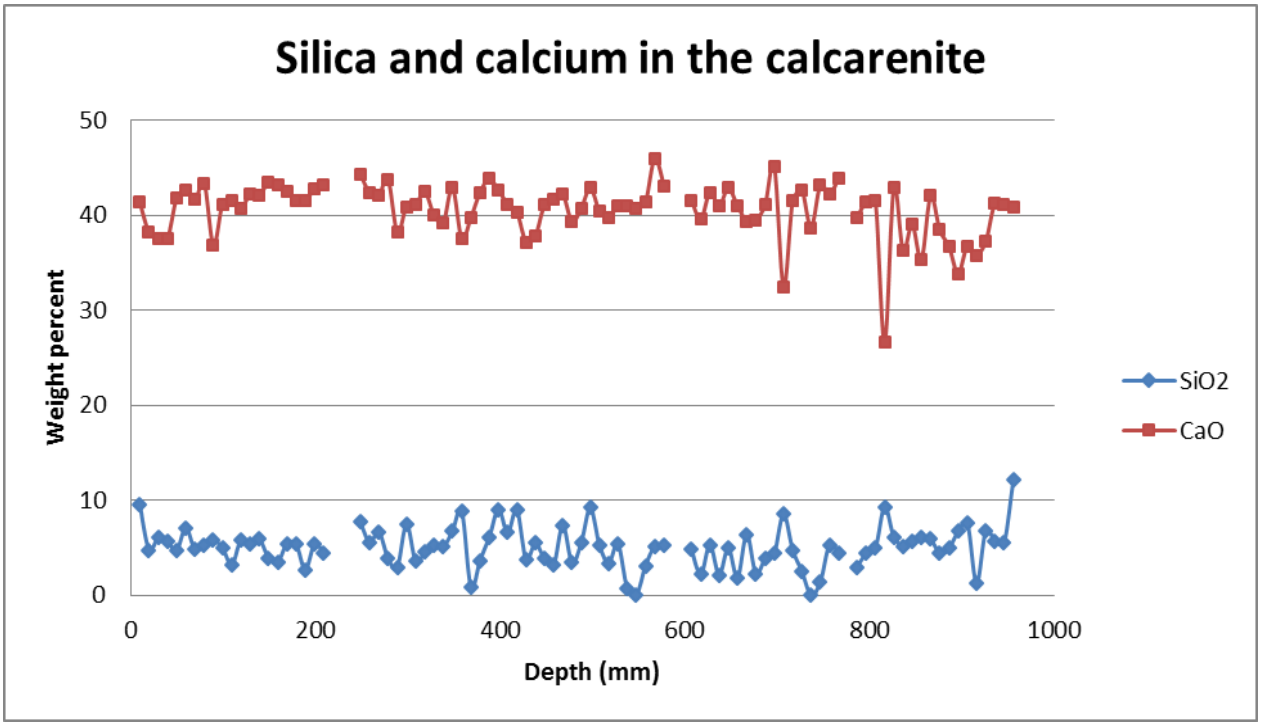

Fig 13. Shows the amount of silica and calcium in one meter of calcarenite (about five meters down). Note that the parts that couldn't be scanned by the ITRAX show up as gaps in the diagram.

4.3.4 Stromatoporoid limestone

The stromatoporoids vary a little in appearance throughout the drill core. Some of them have really sharp boundaries and lot of matrix in between and some are similar to the type example (Fig 14). In this example the stromatoporoids display a gradual boundary and grow almost intertwined at times. In the picture below, the lighter beige parts are thought to be stromatoporoids whereas the darker parts are a calcarenite matrix.

The chemical data on the stromatoporoid limestone is overall uniform with a CaO of about 41 % (table 8). There are some noticeable low values and a few peaks (Fig 15). The SiO_2 values vary more but generally lie a bit below or just above 5 %.

Table 8. Shows the average, range and standard deviation (in weight percent) of SiO_2 and CaO in stromatoporoid limestone

	SiO_2 Weight %	**CaO Weight %**
Average	4.03	41.06
Range	0-13.68	24.07-46.1
Standard deviation	2.59	2.70

Fig 14. A sample of stromatoporoid limestone from the core (about ten meters down). The stromatoporoids are light beige in the picture.

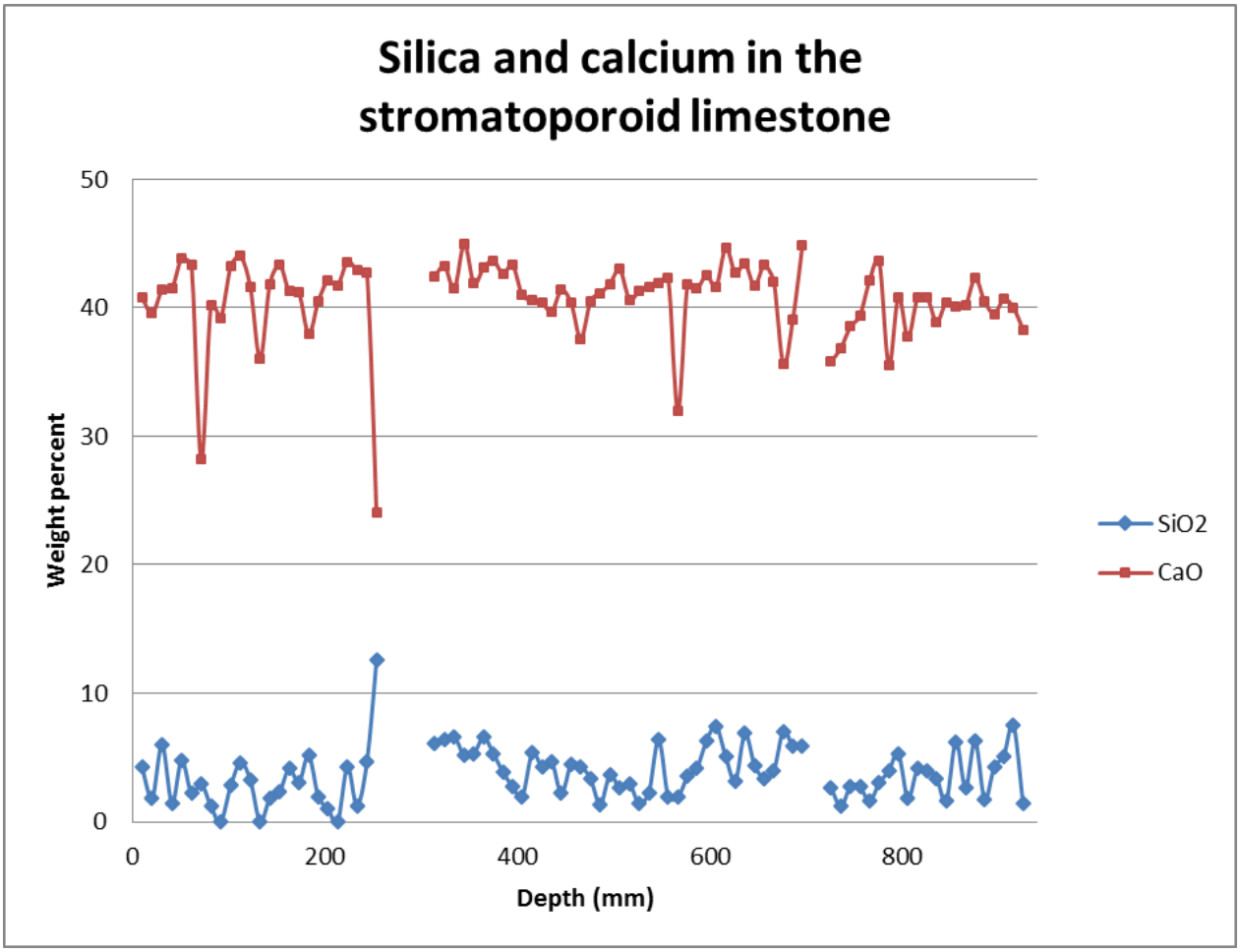

Fig 15. Shows the amount of silica and calcium in ca 90 cm stromatoporoid limestone (about one meter down). Note that the parts that couldn't be scanned by the ITRAX show up as gaps in the diagram.

4.3.5 Fragment limestone

The typical fragment limestone is dominated by fossil fragments surrounded by a micrite matrix (Fig 16). The fossils are usually made up by crinoids and stromatoporoids but sometimes also bryozoans. The fragments themselves vary in size and are generally poorly sorted. The matrix is usually argillaceous and has a greyish, sometimes almost green colour.

The fragment limestone has variable values for both SiO_2 and CaO and the curves for the two elements are different for different parts of the core (Fig 17). However no matter where you are in the core, the SiO_2 content is around 6-7 % and the CaO around 38 % in the fragment limestone (table 9).

Table 9. Shows the average, range and standard deviation (in weight percent) of SiO_2 and CaO in fragment limestone.

	SiO_2 Weight %	**CaO Weight %**
Average	6.50	38.14
Range	0-21.11	20.84-46.48
Standard deviation	4.19	5.62

Fig 16. A sample of fragment limestone from the core (about 6 m down).

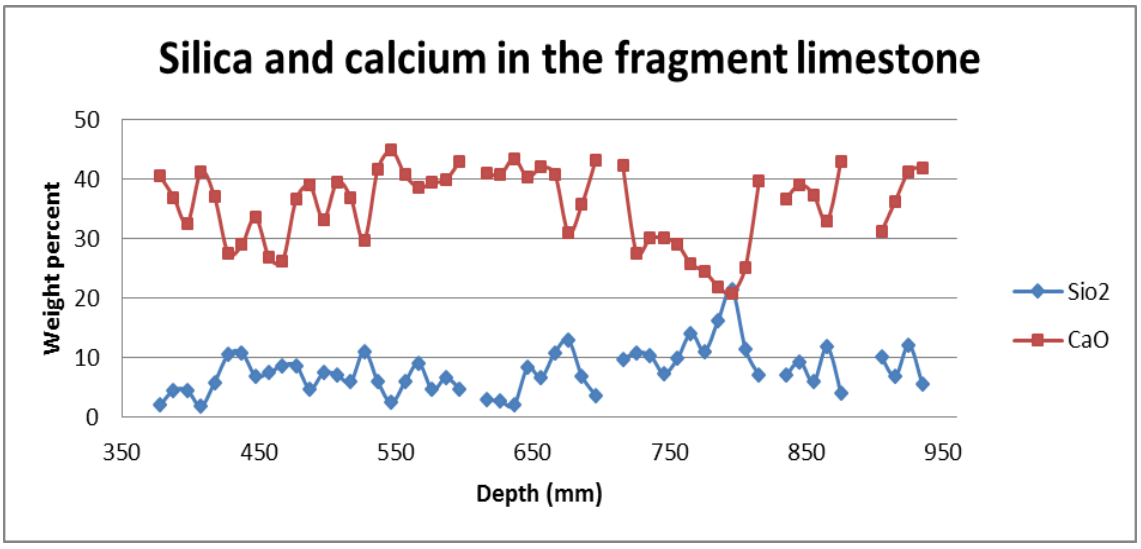

Fig 17. Shows the amount of silica and calcium in 60 cm fragment limestone (about six meters down). Note that the parts that couldn't be scanned by the ITRAX show up as gaps in the diagram.

4.3.6 Reef limestone

There is only one interval (24-25 m) in the core where there is reef limestone. Most part of the reef limestone is made up of stromatoporoids. These grow very tightly, sometimes on top of each other, with no matrix between them (Fig 18). Some 10-20 cm thick interlayers, however, are dominated by crinoids rather than stromatoporoids. Sometimes there are pockets of marl within the stromatoporoids themselves (Fig 19) but these are usually only a few cm big.

The reef limestone shows not only the single highest CaO value but also has the highest CaO average in general 42.5 % (table 10). The SiO_2 content varies greatly, compared to the CaO content, which is more stable with only a few anomalies (Fig 20), and has an average of 6.26%.

Fig 18. A sample of reef limestone from the core (about 24 m down).

Table 10. Shows the average, range and standard deviation (in weight percent) of SiO_2 and CaO in reef limestone.

	SiO_2 Weight %	**CaO Weight %**
Average	6.26	42.53
Range	0-18.62	25.72-48.11
Standard deviation	4.36	3.22

Fig 19. A sample of reef limestone from the drill core (about 24 m down). A typical marl-pocket is marked with red.

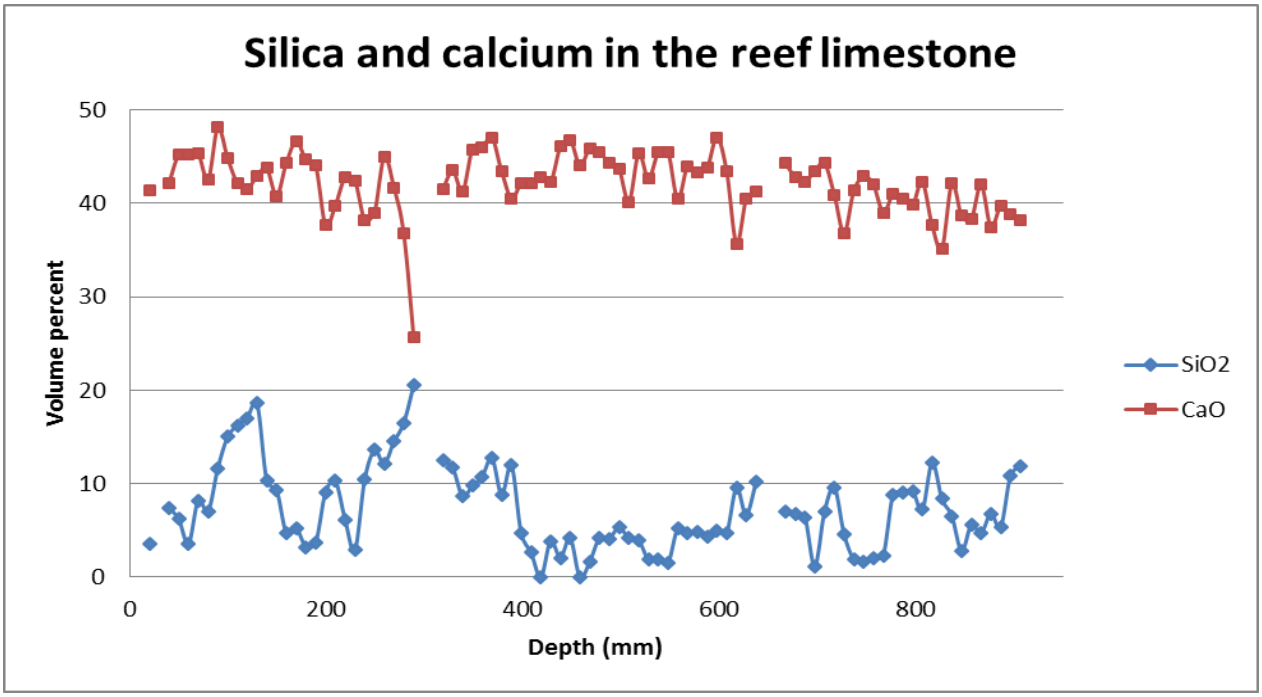

Fig 20. The amount of silica and calcium in ca 90 cm reef limestone (about 24 m down). Note that the parts that couldn't be scanned by the ITRAX show up as gaps in the diagram.

4.4 Handheld XRF

The handheld XRF data was used to see if the core's geochemistry is similar to other studies from Gotland. Here Si, Al, Fe, Mn, Mg, Ca, P, S, V, Cr, Ni, Zn, Ti, Cu, Rb, Sr, Y, Zr, Nb and Ba was analysed. To be able to compare the values of the silica and calcium they had to be recalculated as oxides. Note that strontium and zinc is discussed in the chapter about trace elements and isn't further commented upon here. All other elements, with the exception of barium, corresponded to the values from Cox analytical and therefore will not be discussed either.

It was noted after analysing a pure calcite crystal that the handheld XRF was incorrectly calibrated to CaO and that the received values were higher than the reality. To compensate for this, all values were divided by 1.079. The recalibrated result show that the CaO content is about 53 % (table 11), which is the same as samples from Storugns. The only exception is the fragment limestone, which contains 47 %, and is the only rock type below 50 %. The calcarenite and calcilutite has higher values than the stromatoporoid limestone and slightly higher than the reef limestone.

The SiO_2 content is generally around 1-2 %, which is normal, compared to previous studies of the limestone from the Storugns area (Shaikh *et al.* 1990). Once again the fragment limestone is the exception as it has a SiO_2 content reaching 3.5 %. The calcarenite and calcilutite has lower values of SiO_2, as opposed to the CaO, where it is reversed.

Barium is noted to reach higher values in the data from the handheld XRF compared to the data from ITRAX. The barium content is around 200 ppm in both but in the ITRAX data there are few peaks with long intervals without any barium. In the handheld XRF, however, barium is always found in all points of analysis independently of the rock type. The barium content is generally also greater than in other samples from Storugns, which usually lies around 2-30 ppm.

It was also noted that the amount of magnesium was greater in the fragment limestone than the other rock types (around 10 % compared to around 5 %). Since the amount of magnesium wasn't measured by the ITRAX equipment this cannot be confirmed and the fact that the errors for measuring magnesium is as high as the received values in many cases, the values can only be seen as an indication.

Table 11. Shows the average SiO_2 and CaO (in weight percent) in the different rock types.

	CaO	SiO_2
Fragment limestone	46.95	3.65
Calcarenite	54.03	1.88
Stromatoporoid limestone	52.68	2.41
Calcilutite	54.49	1.29
Reef limestone	53.48	1.96

4.5 Student's t-test

The data from the ITRAX equipment is statistically valid ($P<0.05$) in about 83 % of the cases (table 12). The rock types can always be told apart either by using SiO_2 or CaO but there are some cases in which only one of them can be used. Firstly the student's t-test isn't valid in three cases when SiO_2 is used (20 %). This is when calcarenite-calcilutite, calcarenite-reef and fragment-reef are compared. Secondly the CaO is valid in 87 % of the cases. The only exceptions are stromatoporoid-calcilutite and fragment-marl.

The data from the handheld XRF however can only be used in 65% of the cases and 30% cannot be told apart by neither CaO nor SiO_2 (table 13). The handheld XRF can be used to distinguish between calcarenite-fragment, stromatoporoid-calcilutite, stromatotporoid-fragment, calcilutite-fragment, calcilutite-reef and fragment-reef, no matter if CaO or SiO_2 is used. Calcarenite and stomatoporoid limestone is only statistically different in CaO whereas SiO_2 cannot be used. Three types of rock cannot be distinguished with either element: calcilutite-calcarenite, reef-calcarenite and reef-stromatoporoid.

Table 12. The p-value from comparing the different rock types using SiO_2 and CaO on the values from Cox analytical. The boxes marked in green are significantly different meaning that the ITRAX can be used

P-value	SiO_2	CaO
Calcarenite- stromatoporoid	0.0032	$7.75E^{-5}$
Calcarenite- calcilutite	0.17	0.05
Calcarenite- fragment	$3.76E^{-5}$	0.0055
Calcarenite- marl	$6.78E^{-8}$	0.039
Calcarenite- reef	0.063	$1.57E^{-9}$
Stromatoporoid- calcilutite	0.0044	0.16
Stromatoporoid-fragment	$6.67E^{-12}$	$5.76E^{-6}$
Stromatoporoid- marl	$1.77E^{-11}$	$1.93E^{-8}$
Stromatoporoid- reef	$4.31E^{-5}$	$3.29E^{-6}$
Calcilutite- fragment	$5.21E^{-6}$	0.00048
Calcilutite- marl	2.91E-^{9}	$5.21E^{-9}$
Calcilutite- reef	0.0013	$5.23E^{-5}$
Fragment- marl	$4.37E^{-8}$	0.11
Fragment- reef	0.19	$1.29E^{-8}$
Marl- reef	0.0051	$2.17E^{-9}$

Table 13. The p-value from comparing the different rock types using SiO_2 and CaO on the values from the handheld XRF. The boxes marked in green are significantly different.

P-value	SiO_2	CaO
Calcarenite - stromatoporoid	0.068	0.0023
Calcarenite - calcilutite	0.056	0.15
Calcarenite - fragment	$7.32E^{-6}$	$7.78E^{-8}$
Calcarenite - reef	0.092	0.49
Stromatoporoid - calcilutite	0.010	0.00095
Stromatoporoid - fragment	0.00060	$5.82E^{-7}$
Stromatoporoid - reef	0.087	0.14
Calcilutite - fragment	$1.96E^{-6}$	$7.70E^{-8}$
Calcilutite - reef	0.042	0.014
Fragment - reef	0.00015	5.4E-09

4.6 SEM

The residual material from the acid dissolution of the core samples contained mostly the same mineral phases; traces of calcite which hadn't dissolved, pyrite, quartz, k-feldspar, albite and aggregates of clay minerals. Some of these are illustrated in figure 21. In the calcilutite small amounts of barite, $BaSO_4$, was found. In addition sphalerite, (Zn,Fe)S, was found in the calcarenite, stromatoporoid limestone and fragment limestone. Furthermore arsenopyrite, FeAsS, was found in small amounts in the stromatoporoid limestone. Lastly the quartz in the calcilutite had a different structure compared to detrital quartz and looked almost like a sponge (Fig 21).

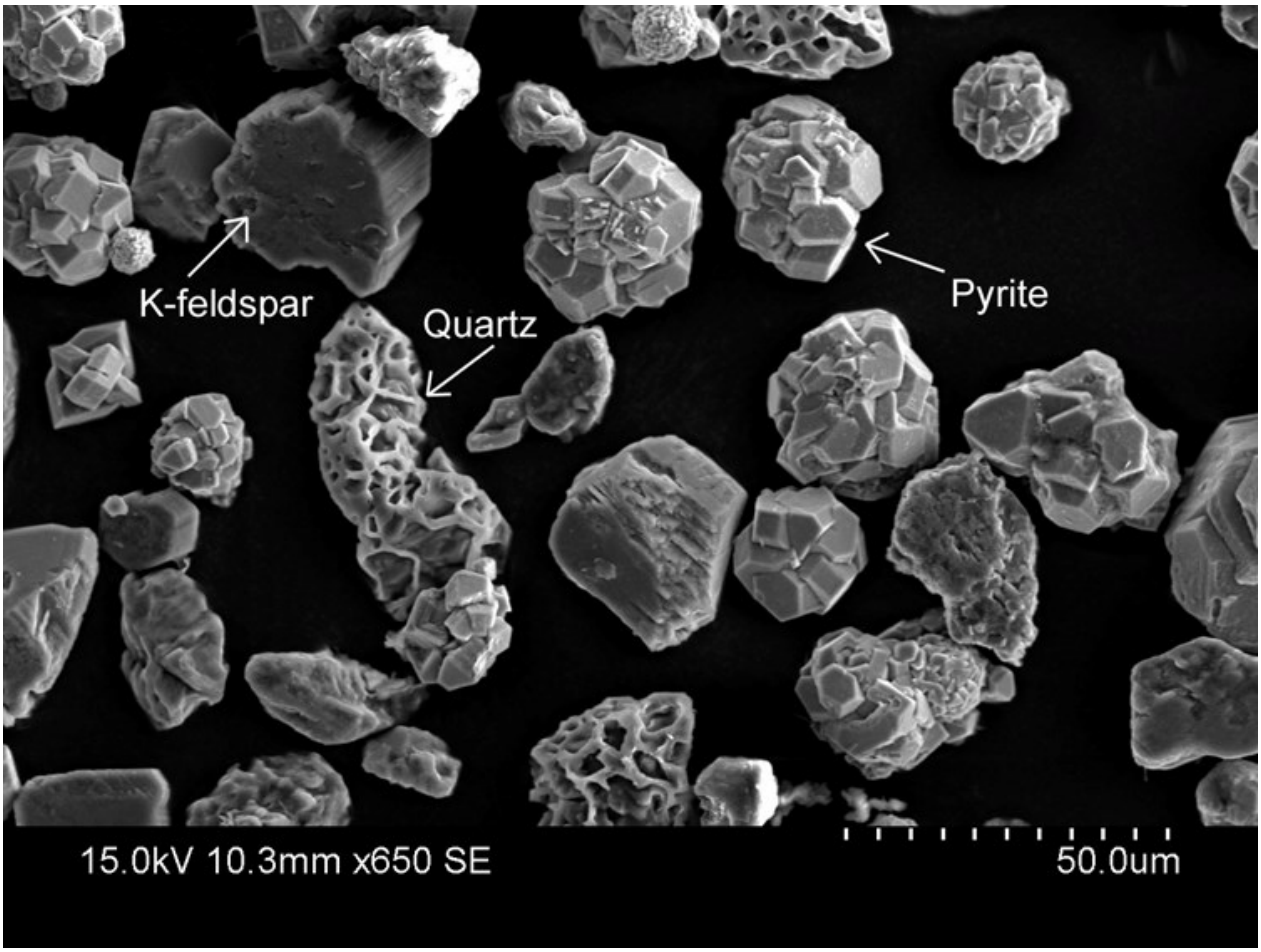

Fig 21. A SEM picture showing the most common residual mineral phases, except for calcite, of the drill core. Note the sponge-like appearance of the quartz.

5 Discussion

5.1 Chemistry

5.1.1 Major elements

The amount and occurrence of the major elements seems to be mostly associated to the relation between the amount of terrigenous minerals and carbonates in the rock. Therefore most of the elements relate to the amount of these mineral types present. The calcium is almost exclusively associated to carbonates in detrital fossil fragments, authigene crystallisations (sparite) and as minute clays sized particles (micrite). The occurrence of other main elements beside calcium is almost exclusively related to amount of sediment originating from land i.e. terrigenous clastics such as clay minerals, quartz and feldspars. The exceptions are the less common major elements, such as sulphur. This might be because the bulk of these elements aren't the result of sediment influx but rather that they exist in other minerals than calcite that are naturally precipitated in the waters (like barite), related to some fossil groups or that some of the elements (such as strontium) can take up places in carbonate minerals.

As stated before, the amount of calcium is connected to the type of limestone and the types that contain clay rich sediments usually show a lower amount of calcium. This is most likely a result of the depositional environment. Rock types that contain a greater amount of land derived sediments, such as calcarenite (which is deposited in front of or behind the reef), will have a higher percent of other elements beside CaO.

The amount of calcium isn't only connected to the rock type itself but is also affected by the presence of lenses of clay and argillaceous stylolite seams. Many rock types, such as the calcarenite and stromatoporoid limestone, show decreasing amounts of calcium connected to the presence of argillaceous stylolite seams. In many cases the decrease can be traced to the clay occurring associated with the stylolite seam, however this isn't always the case. Since not all rock types contain stylolites these might be important and should not be discounted. There's no clear correlation between stylolites and the amount silica. In some cases the silica level rises in a stylolite but there is no distinct pattern of a consistent relationship. Some rock types, such as reef limestone, also contain lenses of marl or clay within fossils, such as stromatoporoids. These may also decrease the calcium levels and give a false reading. However this is not likely to present much of a problem if bigger samples are used.

Normally one would expect an increased amount of sulphur in more argillaceous parts or in clay filled fractures but this does not seem to be the case. However, when looking at the values from the ITRAX scanning, the sulphur levels are normal or slightly higher than normal, sometimes going up to around 0.3 % but with an average of 0.1 %. The average is the same when using the handheld XRF. This indicates that there is indeed sulphur, potentially in pyrite crystals.

Finally the values of the ITRAX scan is affected greatly by the calibrations of the equipment. All comparisons to previous studies are therefore uncertain as this makes the methods used in the different studies too different to compare successfully. This means that the values might be completely normal and only point to the difference how the amounts are measured; however it still seemed valid to note the differences as they might be helpful to future studies.

5.1.2 Trace elements

The amount of trace elements measured in the core display a much greater range of values in comparison to the values previously measured at Storugns. This however might be a moot point since there seems to be no real correlation between where there are peaks of trace elements, as well as their values, and the rock types, which was unexpected. Therefore using trace elements doesn't seem to be a reliable method of distinguishing different types of limestone. Since the data from the ITRAX scanner cannot be used to compare with previous data from Storugns, data from the handheld XRF will be used for the comparison (see below).

It's also worth noting that the values from previous studies might be the average of the entire core, whereas this study has focused mainly on the peaks. Most of the recorded amounts of trace elements are only slightly different from the previous studies when an average for the entire core is used.

5.1.3 Geochemistry of the rock types

5.1.3.1 Marl/marlstone

Although the marl/marlstone display relative high values of SiO_2 and low CaO it's hard to draw any conclusions due to the fact that it exists only in two places of the core and only in a few thin layers. Since the marl was never cut, photographed or analysed with a handheld XRF this also makes the geochemical interpretation of this rock type particularly difficult. The marl/marlstone is lower in CaO than in the previous studies (around 35 % versus 40 %). This is most likely due to the fact that the ITRAX measures the amount differently than the previous studies by Shaik *et al.* (1990). This problem is true for all rock types, as the recorded values are all lower than expected, but especially troublesome for the marl because no handheld XRF was used for comparison (since the marl was too soft to cut). It is possible that this marl/marlstone is in fact a little richer in CaO than what is common due to the fact that it is laminated with calcilutite.

The only case when it is difficult to distinguish marl/marlstone from other rock types, when using the CaO content, is when it's compared with chemical data for the fragment limestone. This is most likely because the fragment limestone contain almost 50 % large fossil fragments and a high amount of micrite and calcareous clay which lower the CaO content and makes geochemically similar to marl/marlstone regarding the CaO content. The silica content can be used however, possibly because the marl contains more clay, whereas the fragment limestone also contains micrite in the matrix.

5.1.3.2 Calcilutite

The calcilutite reflect a low sediment influx from land. The small influx would explain why the silica content is so low. It could possibly also explain why the CaO

content is relatively high. The reason might be that the calcilutite is made up of sediment mainly coming from the reef itself in the form of very fine-grained disintegrated fossil fragments. It is difficult to geochemically distinguish calcilutite from calcarenite and stromatoporoid limestone, especially with the handheld XRF (see below). This can be because calcarenite and calcilutite are largely separated only by the grain-size. With stromatoporoid limestone one faces a similar challenge. Although the matrix of stromatoporoid limestone is usually made up of calcarenite, it can sometimes be made up of calcilutite. This will inevitably make it difficult to distinguish between the two.

5.1.3.3 Calcarenite

The calcarenite is similar to the calcilutite with SiO_2 values just under 5 % and a CaO content of about 40 %. However the calcarenite has a much greater range of SiO_2 values than the calcilutite, probably due to the fact that the terrigenous influx varies more in the area where the sediments building up the rock were deposited. As stated above it's difficult to distinguish calcarenite from calcilutite and calcarenite from stromatoporoid limestone. This is for the same reason as it's hard to tell stromatoporoid limestone from calcilutite; the matrix in the stromatoporoid limestone is usually made up of calcarenite or calcilutite.

5.1.3.4 Stomatoporoid limestone

The stromatoporoid limestone intervals are probably the hardest to distinguish geochemically since the rock type is defined simply by the amount of stromatoporoids and there are parts with a relative high amount of matrix consisting of calcarenite and/or calcilutite.

5.1.3.4 Fragment limestone

The amount and location of different elements in the fragment limestone is strongly connected to the size and frequency of fragments. The amount of CaO, for instance, will decrease significantly in places where there's more matrix. Where there's naturally more clay-rich matrix, the fragment limestone will appear close to the geochemical characteristics of the marl/marlstone. This might also be why it's so hard to distinguish fragment limestone from marl/marlstone and reef limestone. Places where the matrix dominates will have similar signature to marl/marlstone, especially concerning the CaO content, whereas in places where there is less matrix it will be similar to a reef limestone. The fragment limestone is probably also problematic to distinguish from the other rock types because it is defined by the amount of fossils and can be very different in appearance.

5.1.3.5 Reef limestone

The reef wasn't expected to display the highest CaO values as it usually contain pockets and inclusions of finer grained material such as marl. The recorded relative high amounts of CaO may be due to the fact that it contains minor amounts of argillaceous matrix and that is made up mostly of fossils. This is probably not only the reason why the CaO content is so high but also that the SiO_2 is generally low. The few spikes of SiO_2 that exist are mostly associated to stylolite seams or areas where there are lenses of marl within the fossils themselves.

5.2 Handheld XRF

Most of the different rock types show values close to those from previous studies with fragment limestone as the main exception. Here the CaO is lower and the SiO_2 is higher. However since the original data doesn't differentiate between different types of limestone the values may be completely normal. In fact the average of all the rock types is about 52 % which is only slightly lower than in the results presented by Shaik *et al.* (1990). There is of course the risk that this fragment limestone is actually lower in CaO than is normal in previous studies. If that is the case it might be due to a less micrite rich matrix or an overall greater amount of matrix than what is normal.

The calcarenite and calcilutite have higher values of CaO than the stromatoporoid limestone and slightly higher than the reef limestone. This is expected as reef limestone and stromatoporoid limestone often contain small amounts of marl within fossils. The stromatoporoid limestone and fragment limestone contain more SiO_2 than the other rock types. This is most likely also due to the fact that those rock types tend to contain marl. Neither of these things can be seen in the data from the ITRAX scan. However, this might be due to non-representative samples for the handheld XRF or the fact that the data from ITRAX scan is measured differently from the handheld XRF.

The magnesium levels are relatively stable throughout the core but are slightly higher in the fragment limestone. Since the magnesium errors are so high the values themselves are probably not very precise however this still makes it likely that the fragment limestone contains more dolomite.

The data concerning trace elements seems mostly normal compared to previous studies, even though some of them, vanadium for example, is relatively high in comparison to what is expected in the fragment limestone. This might be due to the fact that the handheld XRF measured the values incorrectly or that the fragment limestone contains greater amounts of vanadium compared to other limestones from the same area. The barium spikes in the data from Cox correlate with the amounts from the handheld XRF, however there are very few spikes in the data from Cox compared to the handheld XRF.

5.3 Student's t-test

The data from the ITRAX scan can be used to distinguish the different rock types in 83 % of the cases and if CaO can't be used SiO_2 can. The only problems with using CaO are that the fragment-marl/marlstone and stromatoporoid-calcilutite can't be distinguished. With stromatoporoid-calcilutite the problem might be that the stromatoporoid limestone sometimes contains a calcilutitic matrix. With the fragment-marl/marlstone the similarities might derive from the fact that the fragment limestone contained a high amount of argillaceous matrix which could bring down the overall value of the CaO and bring it closer to that of the marl.

The SiO_2 cannot be used to tell calcarenite-calcilutite, calcarenite-reef and fragment-reef apart. With the calcarenite-calcilutite there is a possibility that the matrix in the calcilutite is made up mostly of

micrite rather than clay minerals. This would not only bring down the SiO_2 values but also increase the CaO, which would make the calcarenite and calcilutite very similar. Regarding the geochemical characterization of the calcarenite and reef limestone the similarity might come from the fact that the calcarenite's matrix is mostly made up of fine carbonate rich sediments and therefore the SiO_2 will be relatively low. The reef contains little matrix and therefore display low SiO_2 contents in general, which might make the two appear similar. Lastly the fragment and reef limestones are quite similar as the main difference is how tightly the fossils are deposited and the fact that both contain argillaceous matrix.

The various limestone types that cannot be geochemically distinguished by the ITRAX scan are quite similar in lithological characteristics and it might not be necessary to be able tell them apart for the industry. Both the fragment and reef limestones for example are usually coarse-grained, which might not be preferable, whereas with calcarenite and calcilutite the potential problems might be more related to the presence of a well crystallised calcite texture rather than the chemical and mineral composition.

The data from the handheld XRF can only be used to distinguish between the rock types in 50 % of the cases and in 43 % they cannot be told apart by using the CaO or the SiO_2 values. First of all stromatoporoid and reef limestone can't be distinguished when using the handheld XRF. This is probably due to the fact that the part of the core chosen as standard for the reef limestone isn't entirely representative. The reef limestone in general has tighter stromatoporoids with marl pockets in some of them whereas the standard's stromatoporoids grow further apart. This makes the reef limestone appear more like a stromatoporoid limestone and therefore they become difficult to separate. This also explains why it works with the data from ITRAX scan. Here the entire reef limestone is used and therefore the difference is more significant. Secondly the calcarenite and calcilutite can't be told apart by using the handheld XRF data or if CaO is used with the data from the ITRAX scan. This could be because the calcilutite in the core isn't pure but contains fragments of fossils which might increase the amount of CaO and make is similar to a calcarenite concerinig CaO. This is especially likely in the handheld XRF as that sample contained more fossils than the rest of the calcilutite. It could also be related to the composition of the matrix, as is discussed above. Thirdly the calcarenite and reef limestone are indistinguishable. This may possible be due to the lack of matrix in them, which makes the SiO_2 levels similar. Lastly the SiO_2 cannot be used to tell stromatoporoid limestone and calcarenite apart. Since the data from the ITRAX scan can be used, one possible reason could be that the sample representing the stromatoporoid limestone contains more argillaceous matrix than the stromatoporoid limestone does in general in the core.

5.4 SEM

The SEM shows that there aren't many accessory minerals in the drill core. The main minerals occurring, except for calcite, are pyrite and quartz but since the performed analysis of the residual material was only qualitative the relationship is not determined. The grains of sponge-like quartz found are thought to have been precipitated in the pore spaces whereas the rest of the quartz is of terrigenous origin. However more studies would be needed to confirm or discard this and as it's not important for this study, it will not be discussed further. The sphalerite found explains why there are some peaks of phosphorous in the geochemical core data. The arsenopyrite is the most unexpected find. Since there hasn't been any records of dangerous arsenopyrite levels in the area before, this find is likely not a problem and might simply be due to the fact that bedrock sometimes contain small amounts of arsenopyrite or possibly that the samples were contaminated while prepared.

6 Sources of error

Since the ITRAX scan differs so much from other chemical analysis methods it's difficult to compare the geochemical data received with those from previous studies. Therefore the handheld XRF was used to get comparable data. However, the handheld XRF contains fewer data points compared to the ITRAX scan, which makes the data less significant. It also increases the risk that the measured data does not fully represent the actual rock type investigated.

The biggest error when it comes to the handheld XRF is how the standard rock types were chosen. They were chosen for practical reasons rather than where the rock was actually representative to the rock type. The problem with non-representative rock types for the handheld XRF may alter the results a great deal since there are few data points per sample. Each rock type only include 20 random spots from a 20 cm long core sample, which only had a diameter of about 40 mm, and the fact that only 20 points per rock type was chosen leads to statistically small test groups, especially compared to the high resolution ITRAX scan. Together the non-representativity and small test groups may affect the results greatly.

Statistics are never entirely reliable and can always be somewhat biased although the validity of results will increase with the amount of data and its quality. Therefore the student's t-test should only be seen as a support and never as actual vertification. In this case for example the statistics point to a reliable method but more studies would need to be done to confirm or disprove that.

7 Conclusions

There are six types of limestone in the core; calcarenite, calcilutite, stromatoporoid limestone, fragment limestone, reef limestone and marl/marlstone. Out of these the stromatoporoid limestone and calcarenite dominate. Stromatoporoids are present in all rock types except in the marl/marlstone and they make up most of the reef and fragment limestones. There are also bryozoans, crinoids and undistinguishable fossil fragments present throughout the core. Many of the layers also contain stylolites and calcite filled fractures and cavities. The more common elements in the core such as silica, iron and potassium have very similar concentration trends but with different magnitudes. The less common elements, such as sulphur, display

sporadic peaks independently of the rock type. The same can be said for the trace elements although most of these show higher values than the values presented in previous studies.

The geochemistry varies between the different rock types identified in the studied core and this is supported by the student's t-test. Firstly the average CaO and SiO_2 varies with the rock type. The highest CaO can be found in the reef limestone, which is unexpected as these rocks usually contain marl/marlstone-pockets. The lowest CaO is found in the marl/ marlstone, which is normal since the marl/marlstone is made up of about 50 % clay minerals. This is also why the SiO_2 is highest in the marl/marlstone. The calcilutite show the lowest SiO_2, which is possibly related to a more micrite-rich matrix. The fragment and reef limestone contain more SiO_2 than the calcarenite and calcilutite, probably because of the marl-pockets and the fact that the calcarenite contain very little matrix. Secondly the variation between the rock types is greater between more different rock types, such as marl/marlstone and reef limestone, which is to be expected. The ITRAX scan seems like a reliable method to distinguish between different rock types, whereas the handheld XRF does not. This might be because the ITRAX scan looked at the entire core and the handheld XRD at minor intervals. This probably means that smaller sample sets yield errors and should therefore be avoided but could also be related to non-representativity of the chosen samples. To avoid these problems the sample should be representative or the sample sizes bigger.

The difference of the rock types is statistically valid in 83% when using the data from the ITRAX scan and if one element can't be used another one can. These points to XRF high resolution scanning being a reliable method but more studies are needed to fully confirm that the method can be used. It's also worth noting that the rock types that can't be told apart are usually quite similar to each other, for example a stromatoporoid limestone with calcilutitic matrix is similar to calcilutite. This might present a problem for the industry but only if that level of detail is needed. The type of rock type a specific industry needs to be able to distinguish therefore defines the possibility to use XRF data, either handheld or with the ITRAX equipment. I suggest doing more tests to try and optimise the method but mostly to see if it can be tailored to match a specific industry's needs.

More tests should be done with a handheld XRF to see if the problem remains even with bigger samples. Preferably to rock types known to be geochemically different. This would also result in statistically more reliable results.

Part 2

1 Introduction

Part II focuses on the potential use of x-ray computed tomography (CT) in petrology and more specifically if CT can be used to analyse the textures and mineralogical properties of limestones. As stated before, Vinnova funded a project in 2014 called *Characterization of physical and chemical properties of carbonate rocks for sustainable and optimized production* (see part 1) where the goal is to increase the general knowledge about the chemical and physical properties of limestone, particularly for the steel industry. One major problem is the formation of fine grained material (fines) during calcination in connection to heating. This problem is also discussed in part 1 but will be looked into further in this part. The goal was to document representative samples and then analyse these with CT to see when and how fractures form when the material is heated to 400, 500 600, 650 and 700 °C. The CT was also tested to determine whether or not it is a suitable method to tell dolomite and calcite apart, as this is also of interest for the industry.

Storugns quarry, operated by Nordkalk AB, produces limestone for the steel industry. It's important that the limestone fulfil certain standard requirements both chemically and physically to be considered usable. A greater knowledge of the limestone properties will guide and facilitate quarrying of compliant qualities and in addition help to avoid unnecessary costs and CO_2 emission for the industry.

2 Background

2.1 Thermal properties of limestone

Like all rocks, limestones are affected when heated. The thermal expansion starts as soon as the rock is subjected to heat but with limestones the effect of the expansion isn't significant until 300 °C (personal communication L. Johansson may 2016). The thermal expansion is caused by the increased temperature which affects the bond length and angles in the mineral, which creates small isolated fractures. At 500 °C the impact of the temperature is greater and fractures start to become connected but it's not until 800 °C that the fractures become truly frequent (Lu-jian *et al.* 2009). For limestones the thermal expansion is especially important since calcite is an anisotropic mineral, meaning that the expansion is different along different crystallographic directions. In calcite the c-axis expands and the a-axis contracts, as opposed to dolomite, which is isotropic and expands in all directions (Luque *et al.* 2011). The presence of an anisotropic mineral means that rock fabric and preferred crystal direction will be especially important factors for mechanic weathering (Siegesmund *et al.* 1999).

Another important thermal factor is the decomposition of minerals. In limestone the two most important minerals are calcite and dolomite. For calcite the decomposition reaction is simple:

$$CaCO_3 \rightarrow CaO + CO_2$$

Calcite ($CaCO_3$) breaks down to burnt lime (CaO) and carbon dioxide (CO_2) when heated, which is one of the reasons why the quality of the limestone is important. The quarrying of higher quality limestone will result in smaller amounts of unusable lime being produced, and this in turn will cause less CO_2 emissions (Johansson 2011). The produced burnt lime is very porous unless it's allowed to sinter at high temperatures. Even though the starting temperature is quite low in theory (provided that the P_{CO2} is low), the decomposition in kilns don't reach economically use-

ful rates until the temperature reaches around 800 °C. This is because the partial pressure of the CO_2 (P_{CO2}) at the reaction site must exceed the total P_{CO2} significantly in the surrounding atmosphere in the kiln for the decomposition to be efficient. This is also the reason why permeability is important; lower permeability requires higher temperatures to compensate for this (Johansson 2011).

The decomposition of dolomite is simple at low P_{CO2}:

$$CaMg(CO_3)_2 \rightarrow CaO + MgO + 2\ CO_2$$

Here the dolomite ($CaMg(CO_3)_2$) breaks down to lime, magnesium oxide (MgO) and carbon dioxide.

At higher P_{CO2} the decomposition has two steps:

$$(1)\ CaMg(CO_3)_2 \rightarrow CaCO_3 + MgO + CO_2$$

$$(2)\ CaCO_3 \rightarrow CaO + CO_2$$

First the dolomite breaks down to calcite, magnesium oxide and carbon dioxide and then the newly formed calcite will continue to break down to lime and carbon dioxide.

3 Method

3.1 Drilling and cutting

First drill cores were prepared by drilling cores with a diameter of 25 mm with a handheld drill (Fig 1). The cores were taken out of four samples representing dolomite-rich limestone from the Storugns quarry at Gotland, and were provided by Nordkalk AB. The cores from each sample where then cut to a length of 25 mm and marked so that each sample was represented by six cores (a total of 20 cores).

3.2 X-ray computed tomography

X-ray computed tomography (CT) was originally developed for medical purposes (Ketcham & Carlson 2001). The uses are less commonly known in geosciences however. CT has only been used in geosciences for about 50 years (Cnudde & Boone 2013) and the possible applications are evolving rapidly. The main restriction in medical science is that the radiation levels must be kept low to ensure that patients are unharmed. This is not necessary for industrial use as the samples tested usually consist of inert material. Therefore industrial CT used in geosciences, usually provides pictures of higher resolution (Ketcham & Carlson 2001). Traditionally so called serial sectioning was used to get a 3D view of geological samples but this method is not only time consuming but also destroys the analysed sample. Conversely CT is a faster non-destructive method, making it much more desirable (Ketcham & Carlson 2001).

Fig 1. A picture of the handheld drill used to collect the Samples. Photo: Jessica Jennerheim

3.2.1 Setup and theory

There are four types of CT; conventional, high-resolution, ultra-high-resolution and microtomography. Of these four, medical CT mostly falls into the conventional type, compared to industrial CT, where all four types are applicable (Ketcham & Carlson 2001). However no matter which type is used they all share the same basic principles and parts, which will be discussed briefly below.

Firstly all CT setups collect data to create *views*. Views are measurements taken from a given position of the sample and can be used to create 2D images, so called slices. If these slices are stacked on top of each other 3D images can be created. In order to create views the CT sends x-rays through the sample to detectors, located on the opposite side, which registers them. To generate a 3D image, views must be created of all planes of the sample, which is achieved by either rotating the x-ray source and detectors around the sample or, as is more common in industrial uses, to rotate the sample itself. Depending on the intensity and energy spectra of the x-rays, the quality of the picture will vary. For example, a higher intensity can go through denser material but will generate a higher signal to noise ratio. The x-rays are attenuated while travelling through the sample. Depending on the intensity of the x-ray spectra different processes are responsible for the attenuation. This is important because the result is that low energy x-rays beams are sensitive to differences in sample composition (Ketcham & Carlson 2001).

In this study a 3rd generation CT was used (Model: Zeiss xradia xrm520, Fig 2). Although instead of the usual synchrotron based system, x-ray tubes were used to generate the x-rays and the created beam is cone-shaped instead of the more common fan-shape (personal contact, S. Hall February 2016).

3.2.2 Data visualisation

After passing through the sample, the x-rays reach the detectors. The numbers and size of the detectors influence the overall quality of the results. A sinogram (a single set of detector readings for a view) is created and this is converted to a 2D image. It's these stacked 2D images that make up the 3D image (Ketcham & Carlson 2001). A visualisation software is required to create the 3D images and the program turns the 2D pixels into 3D voxels that can be assigned a specific colour (usually greyscale) depending on its intensity.

The data can then be visualised either by volume rendering (highlights voxels with specific intensities) or isosurface rendering (creating isosurfaces of surrounding segmented volumes) or a combination of both (Fusseis *et al.* 2014).

3.2.3 CT in geology

Even though the applications of CT in geosciences are still being developed there are already several fields in which the technique is useful. For example CT can be used in 3D pore characterisation (Cnudde & Boone 2013). Previously the only 3D information received when characterising pores was from 2D descriptions of individual layers but with today's technology pores can be imaged down to a submicron scale. This can for example be used to see weathering in natural building stones. CT can also be used for grain analysis to compare individual grains and study for example their volume. This can be used to study reservoir properties or sedimentary 3D structures (if the contrast in density is sufficient) among other things. CT is also useful for studying fractures, fluid flow or even geological processes. However to get the best image the sample mustn't be moved during testing and this is seldom convenient as it requires all tests to be done inside the x-ray CT systems. Therefore it's common to remove the sample for tests and then try to align the different 3D images. Fluid flow analysis is possible to do within the x-ray area but the fluid flow must be close to zero during the actual scan to get a good image. One additional example of use is that CT can be used to observe fossils without destroying them, which is especially useful for instance when studying fossilised embryos or animals preserved in amber (Cnudde & Boone 2013).

3.3 CT to find dolomite

In order to see if CT can be used to locate dolomite, a suitable sample containing dolomite was prepared. To confirm that the sample contained dolomite two techniques were used; acid test and scanning electron microscope (SEM). After determining which sample contained most dolomite, this sample was analysed with a CT scan to determine whether the method is good for distinguishing calcite from dolomite.

3.3.1 Acid test & handheld XRF

One of the six cores was taken from each of the four samples from Storugns and put into diluted acetic acid overnight. The calcite will be dissolved by the acid while the dolomite will remain intact. Therefore that the sample containing the most dolomite will be the least dissolved, provided that the samples don't contain many clay minerals.

As a backup of the acid test, the samples were also scanned with a handheld XRF (see part one) to locate the sample containing the most magnesium.

3.3.2 SEM

After selecting the sample assessed to contain the most dolomite, one of the drill cores from this sample was polished, coated with coal and analysed with a scanning electron microscopy (SEM, see also part one). The goal was to locate the amount and occurrence of all mineral phases, dolomite in particular, and to take photos that could be correlated to the CT scan. In order to do this the sample was analysed using EDS and then the backscatter images were saved and assembled as a cross section of the core.

3.4 CT to characterise fractures

The remaining five drill cores from sample 2 were chosen for further analysis. First they were scanned with the CT and afterwards each core was heated to a specific temperature. In order to make the conditions of the test reasonably similar to an industrial calcination, the sample was first heated with a speed of 10 °C per minute up to 200 °C and stabilised there for 20

Fig 2. The CT scanner used in this study. Photo: Jessica Jennerheim

minutes. Then it was heated to the desired temperature with a speed of 5 °C per minute and kept there for one hour. Afterwards the sample was allowed to cool slowly. The temperatures used were: 400, 500, 600, 650 and 700 °C. After heating the cores were once again analysed with the CT scanner. Since calcination is so extensive at 700 °C, the sample heated to this temperature had to be scanned on the same day that it was heated. This was to minimise the risk of reactions between the sample and H_20 and CO_2 in the atmosphere that could affect the core and thus the results.

The resulting images from the CT scan were then stacked and analysed in a program called Fiji ImageJ. In Fiji ImageJ five levels were chosen with regular intervals in the unburnt samples and the corresponding levels were located in the burnt samples. Each level was then compared and all fractures, including old healed fractures were marked using Adobe Photoshop on both the before and after images. The fractures formed from the heating were also measured using Fiji ImageJ and an average length was calculated for each temperature.

4 Results

4.1 CT to find dolomite

4.1.1 Acid test & handheld XRF

After one night in acetic acid the cores were extracted and analysed visually. There is a difference in grain size and fossil content between the analysed cores. The cores from sample three and four are coarse grained with large fossil fragments while the cores from sample one and two are more fine grained and hardly contain any fossil fragments at all. All of the cores were dissolved, although to a slightly different extent (Fig 3), but there was no clear indication that the remaining rock was dominated by dolomite. Therefore this method was discarded from further use.

4.4.2 SEM

Figure 4 shows the drill core that was analysed in SEM (one of the five cores from sample 2). The core seems to be mostly crystalline but with some fossil fragments.

In the backscattered pictures from the SEM analysis, two phases can be seen; one light and one dark grey (Fig 5). Using the EDS, the light grey phase was determined as calcite, which dominates the sample. The dark grey phase was established as dolomite and estimated to make up about 30 % of the sample. Together these two phases dominate the sample almost exclusively but there are some other mineral phases as well. One example is small amounts of pyrite, which can be seen as a white phase in the SEM picture (Fig 6). There are also small amounts of a black phase, which is thought to consist of pore spaces or small fractures.

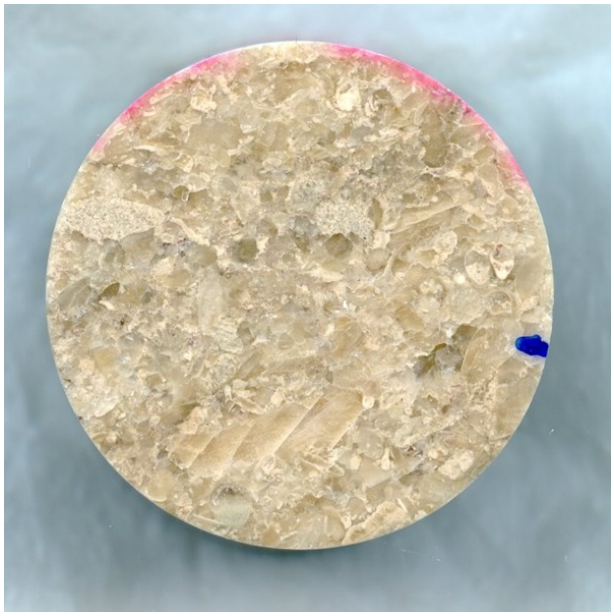

Fig 4. A photo of the core that was scanned in the SEM before being coated with coal. Diameter of the core is around 2.5 x 2.5 mm. Photo: Jessica Jennerheim

Fig 3. The four dissolved samples (one to four from the left). Note the difference in grain size and fossil content. Photo: Jessica Jennerheim

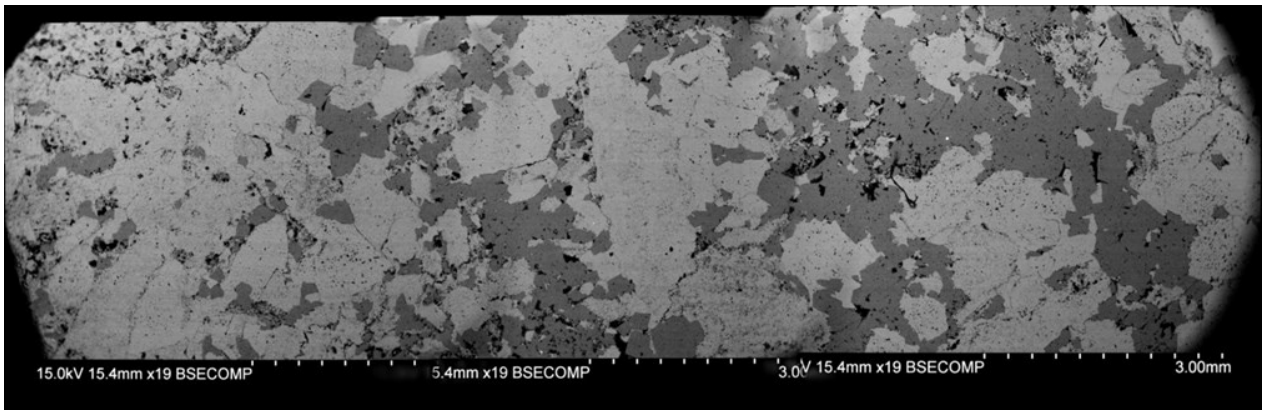

Fig 5. A cross section of backscatter images from the SEM showing the analysed core. The light grey phase is calcite and the dark grey dolomite.

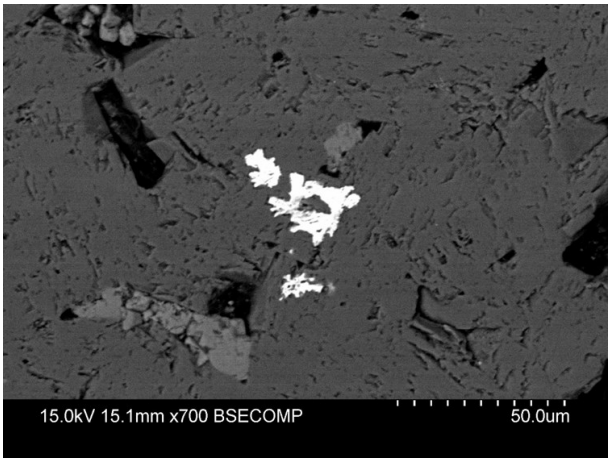

Fig 6. A backscatter photo from the SEM showing a mineralisation of pyrite (white) surrounded by dolomite (dark grey) and minor amounts of calcite (light grey).

4.4.3 CT

The CT scan shows two primary phases, much like the SEM. However it was very hard to find the corresponding level of the SEM picture in the CT scan since the two phases didn't seem to correlate with the confirmed calcite and dolomite in the SEM pictures. One area in one level of the CT scan correlates but otherwise the phases aren't very similar. Since the timeframe was too short, no further attempts were made to use CT to differentiate between dolomite and calcite.

4.5 CT to characterise fractures

Even though the five cores were taken from the same sample they were still somewhat different in appearance and therefore each core will be described shortly. However the images from all cores show two primary phases, one darker and one lighter, in varying abundance. There is also one completely black phase although it's not very abundant. This black phase is most likely porosity and will therefore not be discussed further.

It was also noted for all temperatures that newly formed fractures mostly formed in the lighter phase or at the contacts between the two and not in the dark grey phase.

One example of pictures before and heating will be shown for each one of the applied temperatures; the rest of the pictures can be seen in appendix 3 -7.

4.5.1 Heated to 400 degrees

The core heated to 400 °C contained fairly large grains and numerous fossil fragments of different sizes. There were already some fractures before heating as well as some long, healed fractures. After heating, the old healed fractures opened up, expanded and in some cases split into new fractures. This is also true to some degree for the pre-existing fractures. In general most new fractures could be related to these pre-existing fractures, healed fractures or grain boundaries, and this is where most of them formed. Compared to fractures related to old fractures, which re-opened and therefore varies a great deal in length, most new fractures were short, few and unconnected. Most of the new fractures were also located at the edges of the core however some were formed around the boundaries of fossil fragments closer to the middle. The before and after pictures of one out of five compared levels of the core can be seen in Fig 7. The length of the newly formed fractures was measured and the average was calculated to 2.66 mm (the averages from all temperatures are shown in table 1).

4.5.2 Heated to 500 degrees

This core also contains large grains but has fewer and somewhat bigger fossil fragments than the one heated to 400 °C. Although it's still most common, newly formed fractures are no longer limited to old healed fractures and grain boundaries. The edges of the core still contain more new fractures than the middle however the fractures do seem to form more unanimously over the entire core than when heated to 400 °C (Fig 8). The new fractures are still short and poorly connected but are more abundant. The average length of the new fractures was calculated to 3.14 mm.

4.5.3 Heated to 600 degrees

Just like the other cores this contains large grains. However the upper parts of the core seem more uniform and contain few fossils. There are no old healed

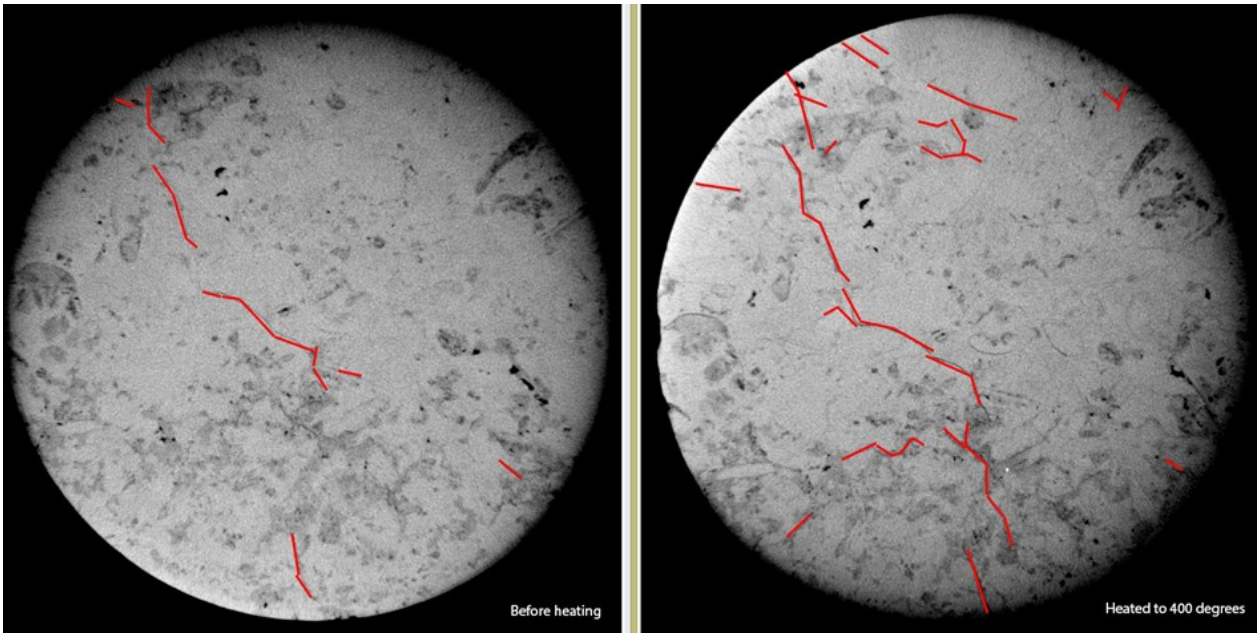

Fig 7. Shows the difference of the limestone before and after being heated to 400 degrees. These pictures are from around 17 mm down in the core.

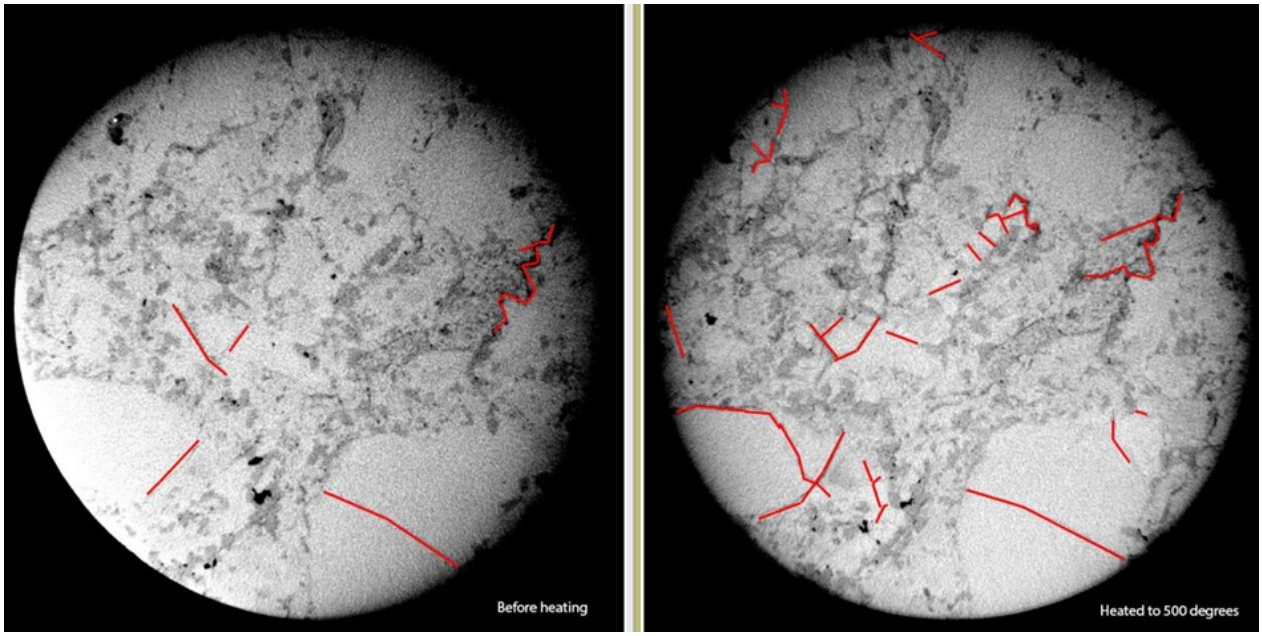

Fig 8. Shows the before and after pictures of the core heated to 500 degrees, taken approximately 17mm into the core.

fractures in the top of the core but there are some very noticeable old fractures towards the bottom. After heating, the top five millimetres of the core show no new fractures at all and it's not until the middle of the core that they become more frequent. Apart from the re-opened fractures there is what looks like a network of small fractures forming in various places of the lower part of the core (Fig 9). These are well connected and located at the edge of the core. Other than these networks there are few new fractures in the core. The average length of the fractures was difficult to determine but was calculated to 2.19 mm.

4.5.4 Heated to 650 degrees

This core is also fairly coarse grained with numerous fossil fragments of varying size. There were also some large fractures already present before heating, generally close to the edges. These large fractures expanded and diverged, creating small, connecting fractures at about 90 degrees from the major crack. There are also several new fractures developed all over the core (Fig 10). They are well connected but do not form any real network. The fractures are no longer only associated only with grain boundaries but are located all over the core, from the edges to the middle. Although the fractures are still mostly associated with grain boundaries they now also seem to penetrate the mineral grains. The average length of the fractures was calculated to 2.76 mm.

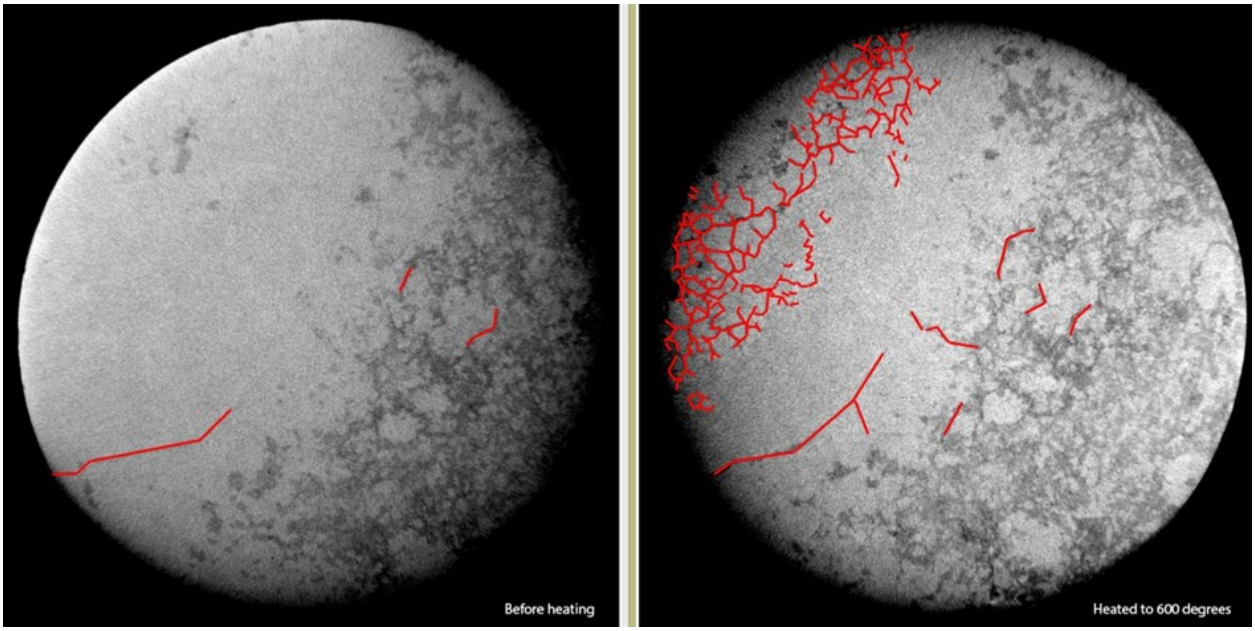

Fig 9. Shows the before and after pictures of the core heated to 600 degrees. Note the network-like fractures toward the edge of the picture to the right.

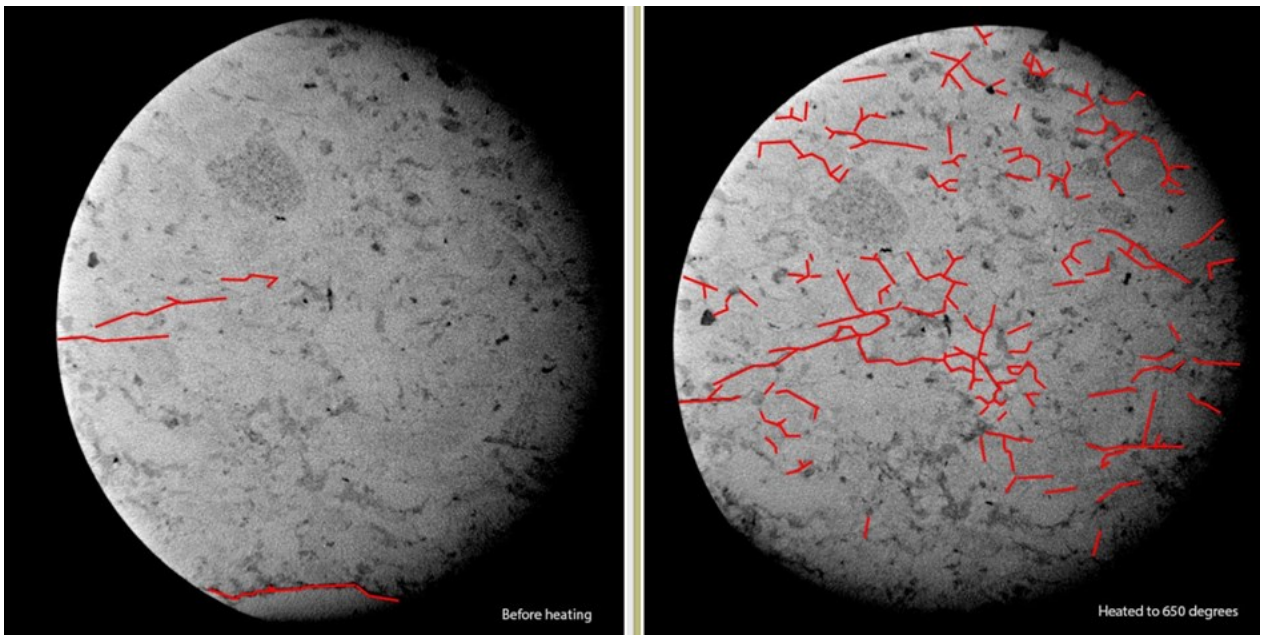

Fig 10. Shows the before and after pictures of the core heated to 650 degrees.

4.5.5 Heated to 700 degrees

This core contains very large grains and few fossil fragments. There are several old, usually long, healed fractures. These opened up as documented for the lower heating temperatures. There are also many new fractures that formed all over the core, independently of grain boundaries and old fractures, although sometimes they are very hard to distinguish (Fig 11). They are generally well connected but there are areas where they do not connect as well. The average length was calculated to 2.65 mm.

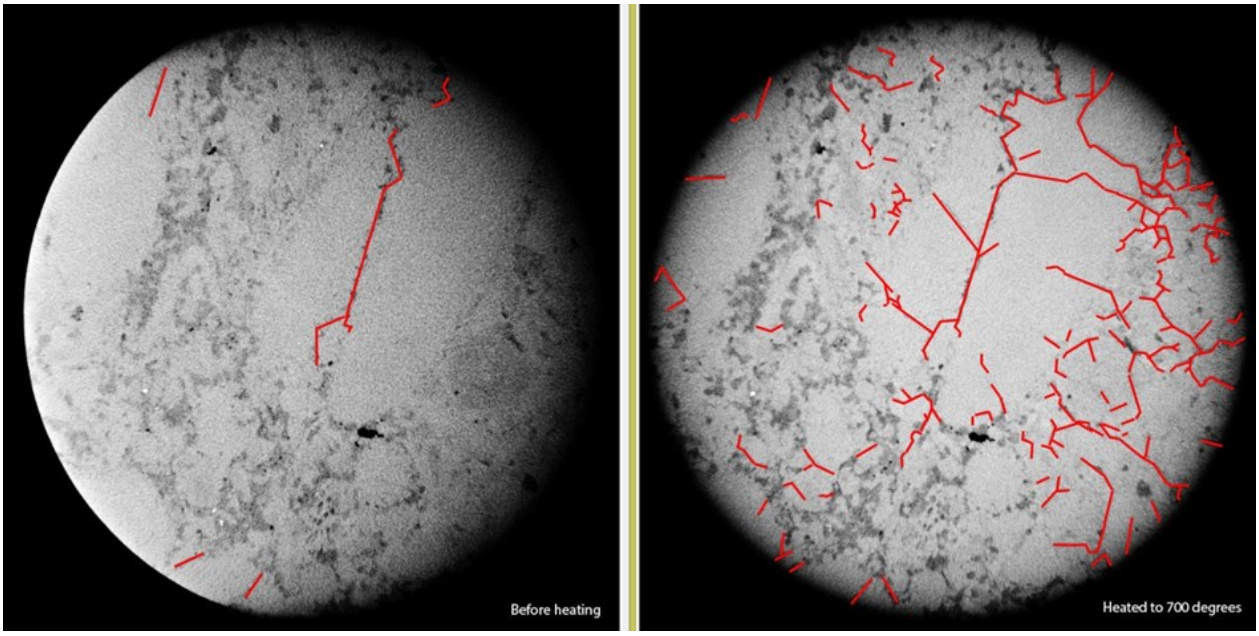

Fig 11. Shows the before and after pictures of the core heated to 700 degrees.

5 Discussion

5.1 Acid test

Since there was no indication that only dolomite remained at the surface after the acid test this method was not used to determine which sample contained the most dolomite. The fact that some samples corroded more than other might be related to the dolomite content, however, it might also be the result of the acid used having slightly different concentration in the different samples. This can also be related to the morphology of the samples since some of them were more crystalline than others and some had greater grain size. If the acid test had been prolonged it's very likely that the calcite had been corroded away and the method could probably have been used but since only an indication of what sample contained dolomite was needed, this method was deemed too slow and uncertain to use. Furthermore a SEM or bulkhead analysis would still be needed to confirm the presence of dolomite which makes this method inferior to a simple test with the handheld XRF. The handheld XRF is therefore not only faster but also more reliable when only an indication of dolomite is required.

5.2 CT to find dolomite

Since the appearance of two phases in the CT scan don't correlate with the phases from the SEM it's hard to tell if the phases seen in the CT are actually calcite and dolomite or simply areas with higher respectively lower porosity. A combination of the two might also be possible, however, it's unlikely that the two phases are solely the result of the location of calcite and dolomite, since if that was the case one would expect the pictures from the CT to correlate better with those from the SEM. One possible way to get better pictures for locating dolomite could be to use smaller samples, which would allow for lower x-ray energies and therefore a more density sensitive result, but this approach was discarded as it would make the samples too small to draw any solid conclusions.

Further testing of CT as a method to distinguish dolomite from calcite was abandoned because of the short timeframe, however it's likely that the method would've worked if more time had been available.

5.3 CT to characterise fractures

It was not only noted that healed fractures opened independently of which heating temperature was applied but also that most of them increased in length and in some cases branched out. The expansion and branching also occurred independently of temperature. This behaviour might be related to the breakdown of the micro spar cement in the old fractures being more sensitive to heating than the bigger calcite or dolomite grains as well as the fossil fragments.

The length of newly formed fractures is generally around 2.6 mm long (see table 1) independently of temperature. There are two exceptions however; 500 and 600 °C. Here the average length is around 3.14 and 2.19 mm respectively. Since these values are only about 0.5 mm from those of the other temperatures this is probably mostly related to normal variation or possibly the measuring being non-exact and is therefore probably not related to the difference in temperature.

Table 1. Shows the average length of newly formed fractures in samples heated to different temperatures.

Temperature (°C)	Average (mm)
400	2.66
500	3.14
600	2.19
650	2.76
700	2.65

There is on the other hand a clear difference in the amount of newly formed fractures depending on the temperature. In the first two temperatures (400 and 500 °C) there are few new, poorly connected fractures that are generally located in grain boundaries or other weak zones, such as old healed fractures. It's worth noting that there is a difference in the amount already between 400 and 500 °C but this is not as great as the difference in higher temperatures. At higher temperatures, such as 650 and 700 °C the fractures become more connected and are not confined to the edges, as at the lower temperatures. This is probably because the furnace affects the edges more than the interior. Therefore the fractures created at lower temperatures are probably a result of the uneven impact from the furnace while heating, whereas at higher temperatures the fracturing is more likely related to calcination. It's also possible that the increased porosity that is usually seen when limestone is heated is related to the fact that the fractures become more connected due to the increased amounts of fractures rather than an increased length and this might contribute to formation of fines.

It was also observed that most new fractures at higher temperatures formed in what looked like finely crystalline light grey areas of the rock. These are thought to be either fossils, possibly fragments of crinoids, or sparite. If it is crinoids the fracturing may be explained by the micro pores of the fossils breaking up but the sparite is equally as likely as the type of structures seen, especially in the 600 °C sample, has been connected to sparite before (personal communication, L. Johansson and M. Erlström may 2016).

6 Sources of error

The newly formed fractures are sometimes difficult to identify, and different monitors show the fractures with different clarity. It's also harder to see new fractures in the dark grey phase, as the colour is closer to that of narrow fractures. This makes the marking somewhat unsure, as some fractures may accidentally be missed or added. This might affect the amount of new fractures counted as well as make the length measurements somewhat imprecise. However this it unlikely to affect the conclusions much as this effect is relevant for all pictures and temperatures and the trends noted are too great for such small differences to alter them. The fact that fractures are sometimes hard to identify might also give the appearance that there are fewer new fractures in the dark grey phase than the light phase even if it might not be true. This might also affect whether fractures look as if they are connected or not and in turn have an impact on the way the fractures are measured.

Another source of error is that the edges of the pictures are not completely aligned with the edges of the actual core. Therefore measuring fractures in this area is harder as the fractures might be longer in reality than they appear in the picture. For this reason these fractures were generally avoided for measuring but in some instances on the lower temperatures, where there are fewer fractures, these were measured anyway to collect more data to analyse.

Lastly the errors for measuring magnesium with XRF, especially a handheld, are great. This mean that sample 2 might not have been the sample containing the most dolomite but since only an indication of dolomite was needed the method was deemed adequate.

7 Conclusions

The acetic test is concluded to be a poor method to indicate dolomite. When only an indication is needed, the handheld XRF is therefore preferable.

Since it was difficult to correlate the SEM picture with the pictures from the CT scan it's been concluded that in order to fully study whether CT scan can be used to distinguish dolomite from calcite or not, further testing would be required.

The CT scanning was determined as a good method to characterise fractures. Lu-jian *et al. (*2009) stated that fractures form as early as 300 °C and the fact that this study show fractures at 400 °C seem to correlate well with those results.

At 400 °C fractures are mainly short and poorly connected. At around 650 °C the fractures become more connected but they are generally not longer than the fractures created at 400 °C. The early developed fractures seem mostly connected to weaker zones in the rock, such as grain boundaries, and they are confined to the edges of the rock. This also changes as the temperature goes up and the fractures seem to form independently of location in the core.

Lastly it's been concluded that the formation of fines is possibly related to the temperature where new fractures begin to connect, about 600-650 °C. However more studies would be needed to confirm this.

8 Acknowledgement

A special thanks to my supervisors, Leif Johansson and Mikael Erlström, at the Department of geology, Lund university, who shared their knowledge and experience. Without your dedication this thesis wouldn't have been possible. Also thanks to Steven Hall and Juan Manuel Paz Garcia from the faculty of engineering, LTH, for all the help with the CT scan and the processing that followed. I also want to thank Anders Rindby from Cox Analytical, who helped me understand the ITRAX equipment and data. Lastly, a thanks to Kenneth Fjäder from Nordkalk AB for providing and helping me with maps from the area.

9 References

Brouwer, P., 2010: *Theory of XRF- getting acquainted with the principles*, pan analytical, ISBN: 90-9016758-7, 3rd edition, 59 p.

Calner, M., 1999: *Stratigraphy, facies development, and depositional dynamics of the Late Wenlock Frojel Formation*, Gotland, Sweden. GFF 121, 13–24 p.

Chen, L-J., He, J., Chao, J-Q., Qiun, B-D., 2009: *Swelling and breaking characteristics of limestone under high temperatures*, Mining Science and Technology, nr 19, pp 503-507

Cnudde, V. & Boone, M.N., 2013: *High-resolution x-ray computed tomography in geosciences: A review of the current technology and applications*, Earth-Science reviews, nr 123, pp 1-17

Erlström, M., Persson, L., Sivhed, U. & Wikström, L., 2009: *Beskrivning till regional berggrundskarta över Gotlands län K221,* 60 p.

Flügel, E., 2004: *Microfacies of carbonate rocks-Analysis, interpretation and application,* Springer, ISBN 3-540-22016-X, 976 p.

Fusseis, F., De carlo, F., Schrank, C. & Xiao, X., 2014: *A brief guide to synchrotron radiation-based microtomoraphy in (structural) geology and rock mechanics*, Journal of Structural Geology, 18 p

Goldstein, J.I., Newbury, D.E., Echlin, P., Joy, D.C., Romig, Jr. A.D., Lyman, C.E., Fiori, C. & Lifshin, E., 1992: *Scanning Electron Microscopy and X-Ray Microanalysis. A Text for Biologists, Materials Scientists, and Geologists*, Second Edition, Plenum Press, ISBN 978-1-4613-0491-3, 840 p

Haynes, W., 2013: *Student's t-Test*, Encyclopedia of Systems Biology, Springer New York, pp 2023-2025, http://link.springer.com/referenceworkentry/10.1007%2F978-1-4419-9863-7_1184 (Available 2016-03-25)

Hede, J.E., 1960: The Silurian of Gotland. *I* G. Regnell & J.E. Hede (red.): *The Lower Palaeozoic of Scania.The Silurian of Gotland*, International Geological Congress XXI, Session Norden, Guidebook Sweden d. Stockholm, 89 p.

Johansson, L., 2011: *Energieffektiv framställning av brända karbonatprodukter – Orsaker till sönderfall,* Lund university, 30 p.

Ketcham, R.A., Carlson, W.D., 2001: *Acquisition, optimization and interpretation of X-ray computed tomographic imagery: applications to the geosciences*, Computers & Geosciences, nr 27, pp 381-400

Kirch, W., 2008: *p Value*, Encyclopedia of Public Health. Springer Netherlands. http://link.springer.com.ludwig.lub.lu.se/referenceworkentry/10.1007/978-1-4020-5614-7_2883 (Available 2016-02-25)

Luque, A., Leiss, B., Álvarez-Lloret, P-. Cultrone, G., Siegesmund, S., Sebastian, E. & Cardell, C., 2011: *Potential thermal expandion of calcitic and dolomitic marbles from Andalusia (Spain)*, Journal of Applied Crystallography, pp 1227-1237

Manten, A.A., 1971: *Silurian reefs of Gotland,* Developments in Sedimentology, nr 13, 537 p.

Olszak-Humienik, M., Jablonski, M., 2015: *Thermal behaviour of natural dolomite*, Journal of Thermal Analysis & Calorimetry, Vol 119, Issue 3, pp-2239-2248

Reed, S.J.B., 2005: *Electron Microprobe Analysis and Scanning Electron Microscopy in Geology*, second edition, Cambridge University Press, ISBN 978-0-521-84875-6, 189 p.

Shaikh, N.A., Bruun, Å., Karis, L., Kjellström, G., Sivhed, U., Sundberg, A. & Wik, N.G., 1990: *Kalksten och dolomit i Sverige. Del 3. Södra Sverige*. Sveriges geologiska undersökning Rapporter och meddelanden 56. 296 p.

SGU, 2014: *Statistics of the Swedish Mining Industry 2014,* Periodiska publikationer 2015:1, 70 p.

Appendix

1.

The amounts of the major elements (in weight percent) from the Slite limestone and marl. * Value below detection limit. Source: Shaikh *et al. (*1990).

Slite limestone (Location)	**CaO**	**SiO_2**	**Al_2O_3**	**TiO_2**	**Fe_2O_3**	**MnO**	**MgO**	**K_2O**	**Na_2O**	**S**
Limestone										
Katrinelund	54.50	0.8	0.36	*	0.21	0.01	0.18	0.11	0.04	0.02
Stutsviken	54.20	0.7	0.41	0.01	0.17	0.02	0.7	0.08	0.03	*
Lansa	55.00	0.4	0.29	*	0.11	0.02	0.3	0.04	0.02	*
Dacker 1 (5 % clay minerals)	51.00	3.1	1.56	0.06	0.72	0.01	1.2	0.48	0.05	*
Dacker 2 (5 % clay minerals)	52.00	2.3	1.18	0.05	0.42	0.02	1.22	0.33	0.05	*
Farnavik	53.80	1.4	0.6	0.02	0.23	0.02	0.71	0.17	0.02	*
Oivide	53.70	2	0.4	0.01	0.4	0.03	0.42	0.13	0.06	0.02
Broa	54.60	0.9	0.42	0.01	0.36	0.03	0.26	0.09	0.03	0.01
Haganäs	49.50	5.4	1.32	0.07	0.66	0.03	1.34	0.4	0.06	0.12
Average	**53.14**	**1.89**	**0.73**	**0.03**	**0.36**	**0.02**	**0.7**	**0.2**	**0.04**	**0.02**
Marl										
Haganäs	33.5	20.7	4.21	0.24	1.42	0.04	4.93	1.51	0.19	0.21
Follingbo	49.6	5.7	1.17	0.05	0.68	0.04	1.19	0.38	0.1	0.18
Munkebos	41.6	12.6	2.69	0.15	1.29	0.13	2.48	0.79	0.21	0.04
Average	**41.57**	**13.0**	**2.69**	**0.15**	**1.13**	**0.07**	**2.87**	**0.89**	**0.17**	**0.14**

2. Core description

0.5-1.66m: Big (5-10 cm) big, massive aggregates with a pink to beige colour. The aggregates are interpreted as stromatoporoids. Around the stromatoporoids there's beige, fine matrix (calcarenite). Within the matrix there's mm-sized fossil fragments and crack-like patterns filled with dark sediments, probably clay. The cracks are thought to be stylolites. The stromatoporoids dominate over the calcarenite but are not intertwined in their structure.

Classification: Stromatoporoid limestone

1.66-2.10 m: Is similar to the overlaying layer but with smaller aggregates (1-3 cm). The matrix is darker and richer in clay. These aggregates aren't as massive as in the layer above and have a more beige colour with fragments of white to pink in them. They are therefore interpreted as fragments of calcarenite. The calcarenite is unevenly layered with a clay matrix.

Classification: Calcarenite

2.10-2.95 m: Is dominated by pink to beige aggregates (3-10 cm) similar to the top layer. These are stromatoporoids. At 2.30 and 2.40 m there are calcite filled cracks. There is little matrix except for the thin layers of clay between the stromatoporoids.

Classification: Stromatoporoid limestone

2.95-5.00 m: Light grey non-massive layers in the sand fraction. These contain small (2-3 cm) red crinoid fragments and other white unidentified fossil fragments. As in the layer above, there are calcite filled cracks (for example at 4.83 m). The light grey areas are crystalline and contain stylolites.

Classification: Calcarenite

5.00-6.17 m: Darker than the overlaying layer. The layer consists of a massive, crystalline and dark grey calcarenite containing small fossils. There are also argillaceous layers with white, unsorted fossils such as crinoids. The last 7 cm of the layer is one big stromatoporoid with a fine greenish matrix around it. The stromatoporoid could possibly be a part of the underlying layer.

Classification: Calcarenite

6.17-7.30 m: Contains many white, beige and pink, unsorted fossils (possibly stromatoporoids. crinoids and bryozoans). Around the fossils there's a dark grey matrix with a green hue, which is argillaceous and feels fatty when touched. The amount of matrix declines in the lower parts of the layer. The fossils are probably fragments of a reef with mud in-between.

Classification: Fragment limestone

7.30-8.00 m: Massive, light beige calcarenite with a sandy feeling to it. Some parts contain stylolites and sometimes the stylolite seams are filled with a grey,

argillaceous matrix. The calcarenite contain many small fossils.

Classification: Calcarenite

8.00-9.85 m: No sharp boundaries in the top or bottom. The layer contains silty, massive areas with mm-sized fossil fragments. Not as beige as the layer above. Between 9-9.10 there is a part that was damaged during drilling. This reacted with the surroundings and developed a yellow surface, possibly from iron or sulfur. The part will be omitted from further studies. There are parts which have a flowy texture. These are dark, argillaceous and contain many unsorted fossil fragment, such as bryozoans. The layer also contains stylolites with brown clay (compared to the clay in the previous layer. which was lighter). To form the flowy part the rock probably went through diagenesis.

Classification: Calcilutite

9.85-11.57 m: Dark grey areas with particles in the sand fraction. These contain beige rounded shapes with blurry edges. They are interpreted as stromatoporoids and are very abundant. Cracks form easily in places where there are clay filled stylolite seams. This makes it hard to see if the fracture surfaces look crystalline. The stylolites are abundant and of different size and colour. Most of them are green and fatty but in the lower parts some are homogenous and grey.

Classification: Stromatoporoid limestone

11.57-17.17 m: Calcarenite with fossil fragments in the sand fraction, usually crinoids. There are also a few bigger fossils which are interpreted as stromatoporoids and bryozoans. The calcarenite is grey and periodically the crystallinity is clearly visible in fractures. It contains a great amount of stylolite seams of different size which are filled with dark grey, argillaceous sediments. Some parts of the layer are coarser and are interpreted as calcirudite. The lower boundary is very sharp.

Classification: Calcarenite with layers of calcirudite

17.17-19.10 m: Beige, massive stromatoporoids with a grey, grainy calcarenite in-between. Thin layers of clay can be found in areas where the two meet. Close to being a reef limestone.

Classification: Stromatoporoid limestone

19.10-19.30 m: A thin layer of clearly laminated calcarenite. Light beige with a small hint grey of in colour.

Classification: Calcarenite

19.30-21.59 m: Light grey with a pinkish hue, massive with abundant small (mm-sized) fossil fragments and a few larger fossils. The layer contains many stylolites with a green, argillaceous matrix. There's no matrix except in stylolites and in the margins of bigger fossils. Parts of this layer contain crystals in the calcirudite fraction. The layer also shows a clear crystallinity.

Classification: Calcarenite with layers of calcirudite

21.59-22.10 m: Dark grey layer containing more matrix than the layer above. There's also many small, unsorted fossils and tiny pyrites in fractions.

Classification: Calcarenite

22.10-22.67 m: Can be divided into three parts. The first part is 10 cm calcirudite with unsorted fossil fragments and as argillaceous, green matrix. Here you can find bigger parts of corals. The second part is a 50 cm laminated calcarenite with little matrix. There are a few bigger fossils here as well and in the end. 8 cm unsorted fossils such as stromatoporoids. The calcarenite gradually changes into a relatively massive, light grey calcilutite containing crinoids and few bigger fossils.

Classification: Calcirudite to calcarenite to calcilutite

22.67-23.50 m: Dark grey, somewhat laminated layer with abundant small fossil fragments and few bigger fossils such as crinoids. The lighter parts of the laminae are fine-grained calcilutite (close to calcarenite) and crystalline while the darker, greenish parts consist of argillaceous marl with a few coarser fragments. This entire layer is homogenous without any stylolites and the last 22 cm contain calcilutite without any marl.

Classification: Marlstone with layers of calcilutite

23.50-25.27 m: Big pink to beige stromatoporoids with little to no greenish matrix in the clay fraction. There are also some isolated spots of marl within the stromatoporoids. The stromatoporoids seem to almost grow together and is probably part of a bioherm. Some layers are made up of crinoids rather than stromatoporoids. These also contain a grey, almost blue, content which might be another fossil. It doesn't feel like clay but cannot be determined as a fossil as of this time

Classification: Reef limestone

25.27-26.10 m: A layer of 27 cm grey and massive calcarenite, with small fossil fragments and a few bigger fossils. Then there's 30 cm which alternates between 10cm green marl to 10cm calcilutite and back to marl again.

Classification: Calcarenite to marl and calcilutite

26.10-28.00 m: starts with 30 cm light grey to beige calcilutite with a few big fossils (3-5 cm) followed by calcarenite with stromatoporoids (5 cm).

Classification: Calcilutite to calcarenite

20-end of drill core: Looks similar to the layer above but is more dominated by fossils, mostly stromatoporoids (about 5 cm) with a calcilutite matrix. The stromatoporoids are oval, compared to the layers above, which have a more rounded shape.

Classification: Calcilutite

3. The before and after CT pictures of the sample heated to 400 degrees. Fractures are marked in red.

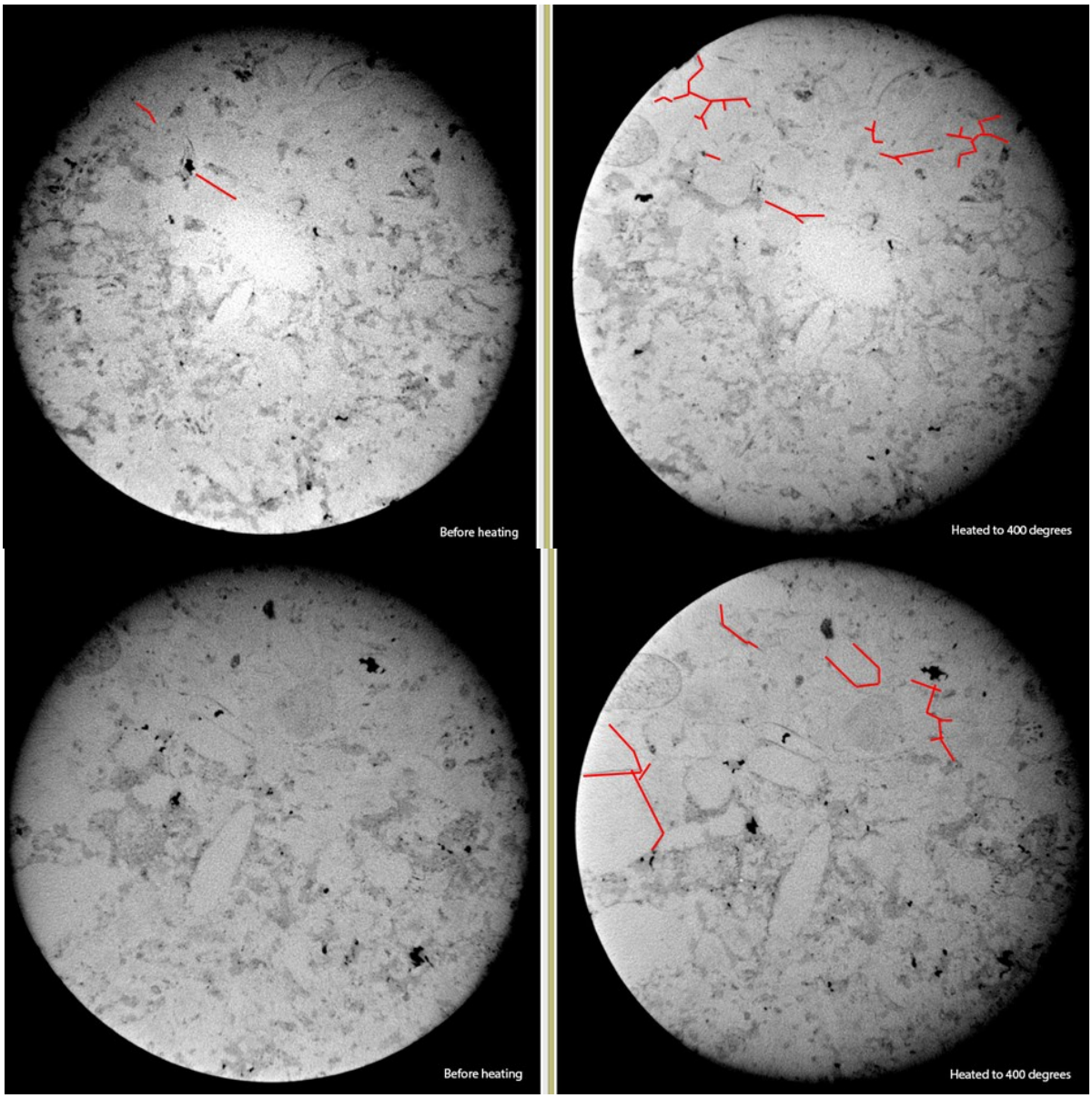

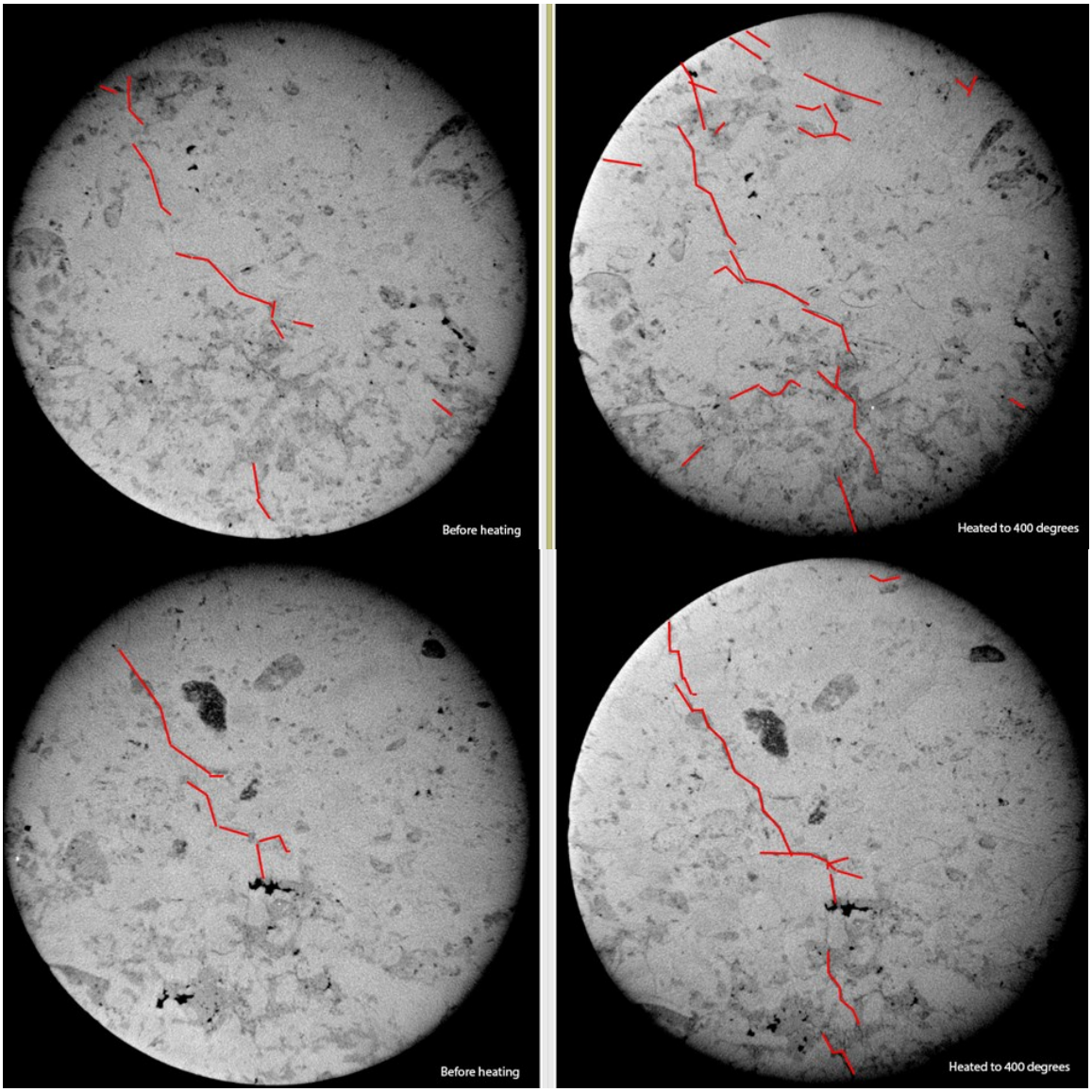

4. The before and after CT pictures of the sample heated to 500 degrees. Fractures are marked in red.

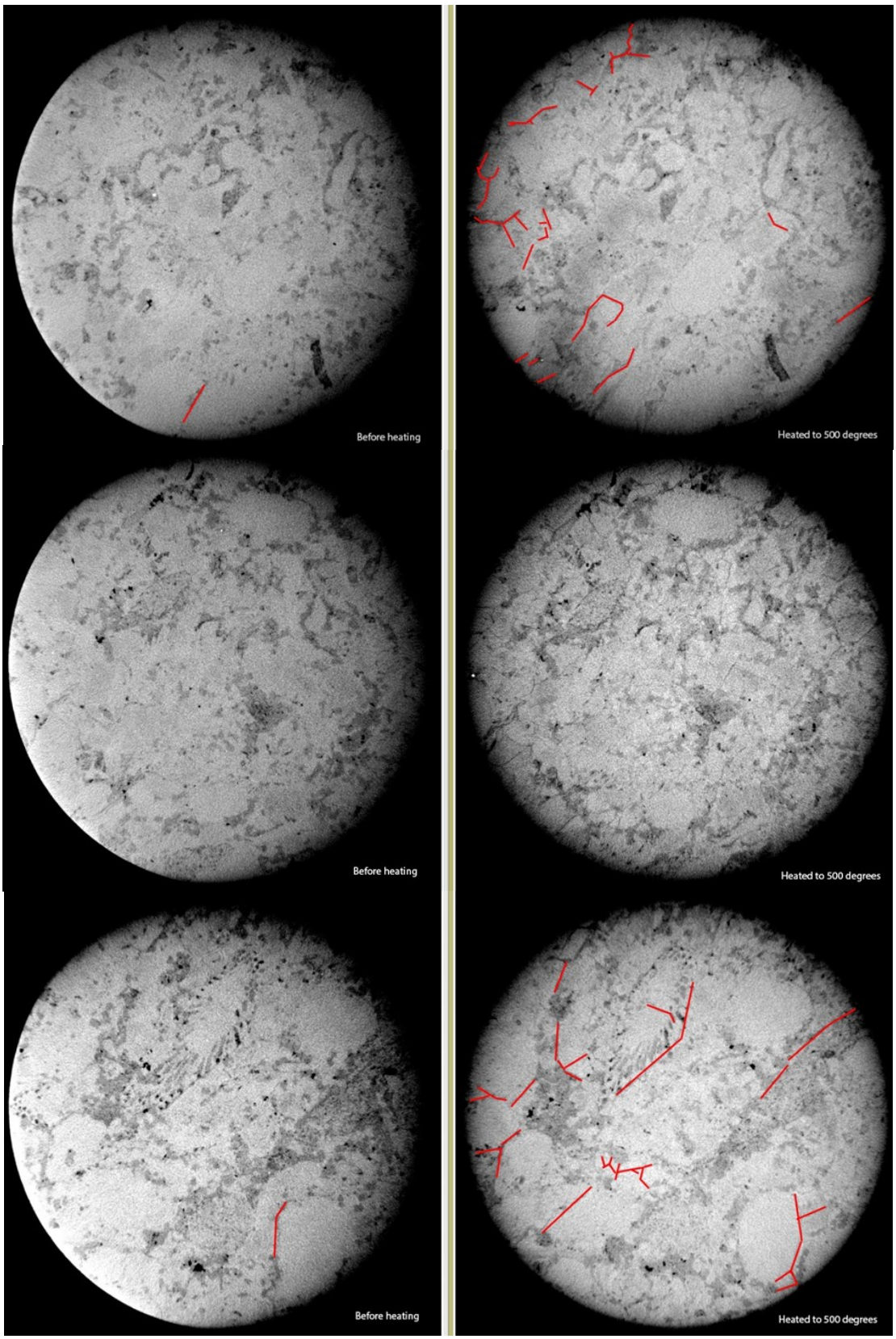
Before heating
Heated to 500 degrees
Before heating
Heated to 500 degrees
Before heating
Heated to 500 degrees

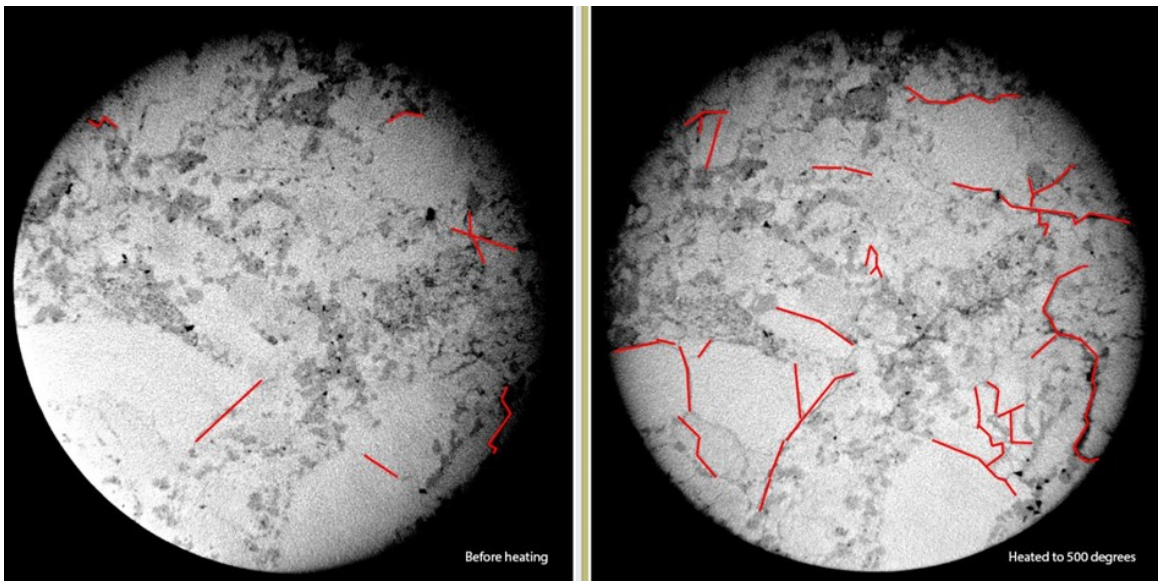

5. The before and after CT pictures of the sample heated to 600 degrees. Fractures are marked in red.

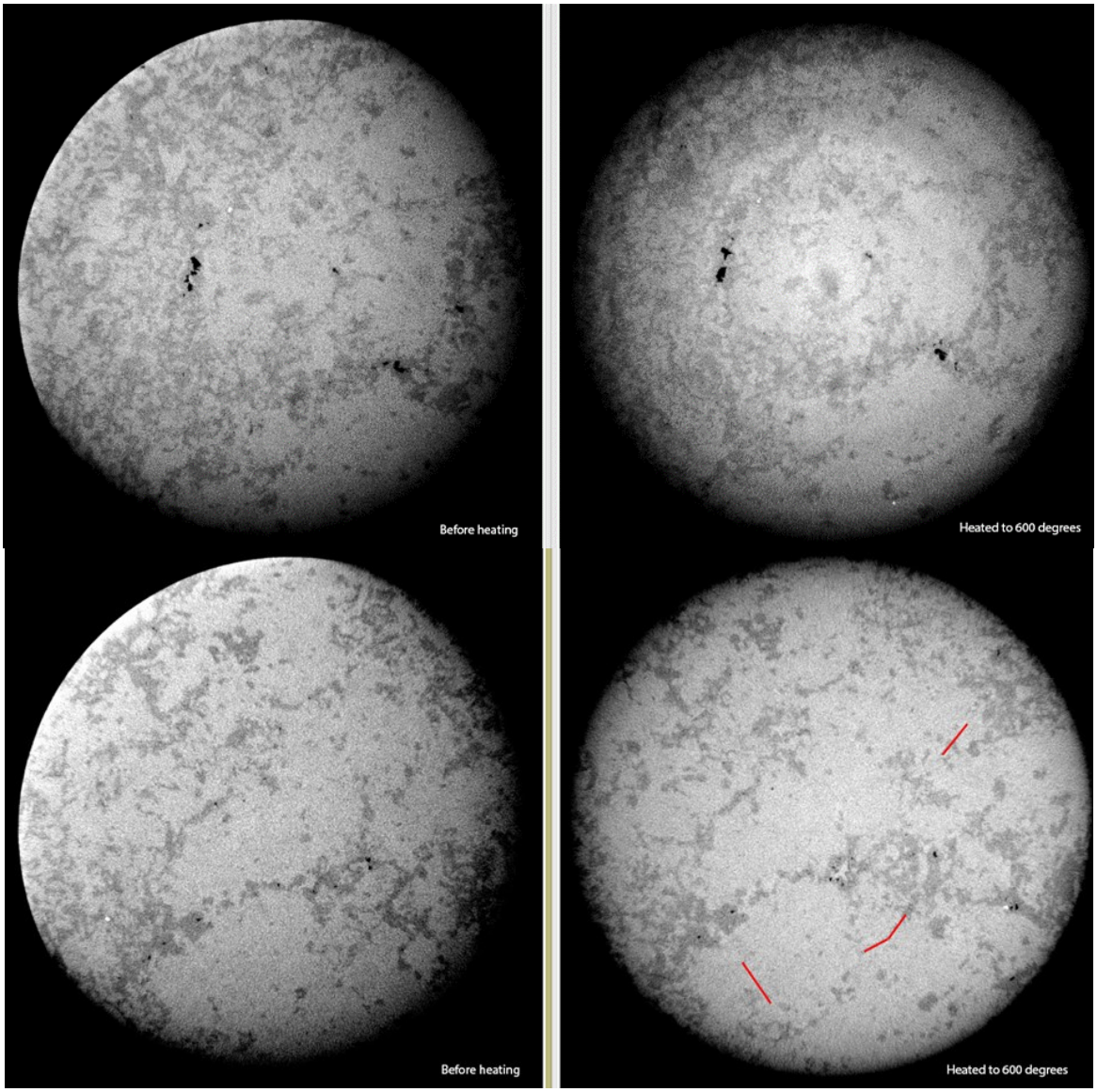

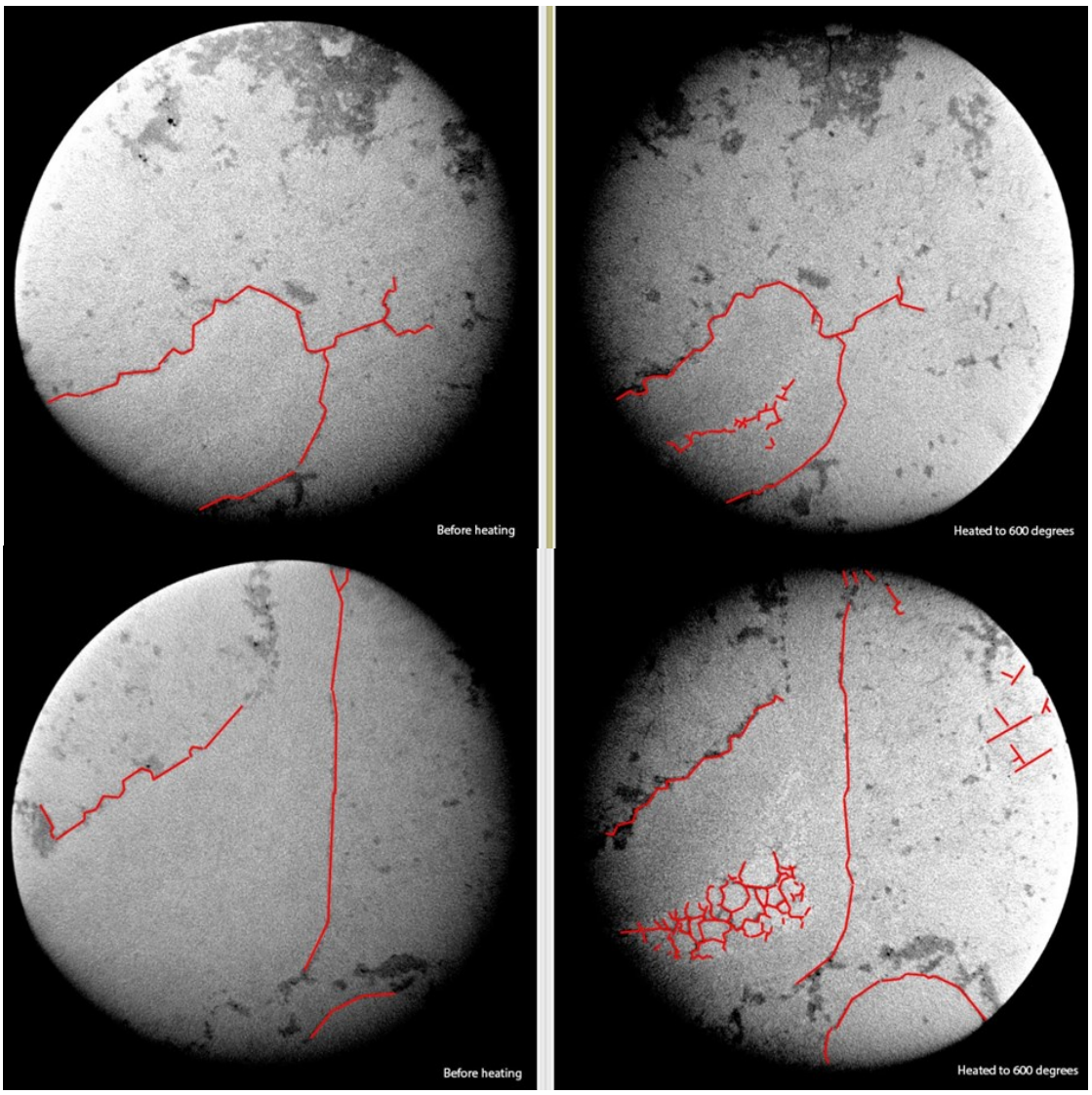

6. The before and after CT pictures of the sample heated to 650 degrees. Fractures are marked in red.

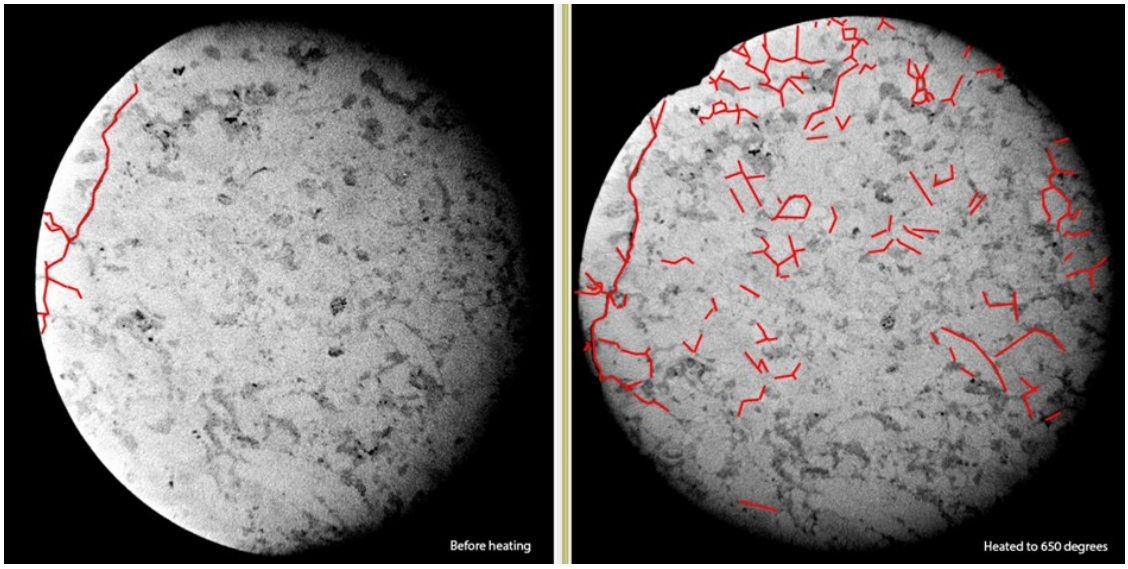

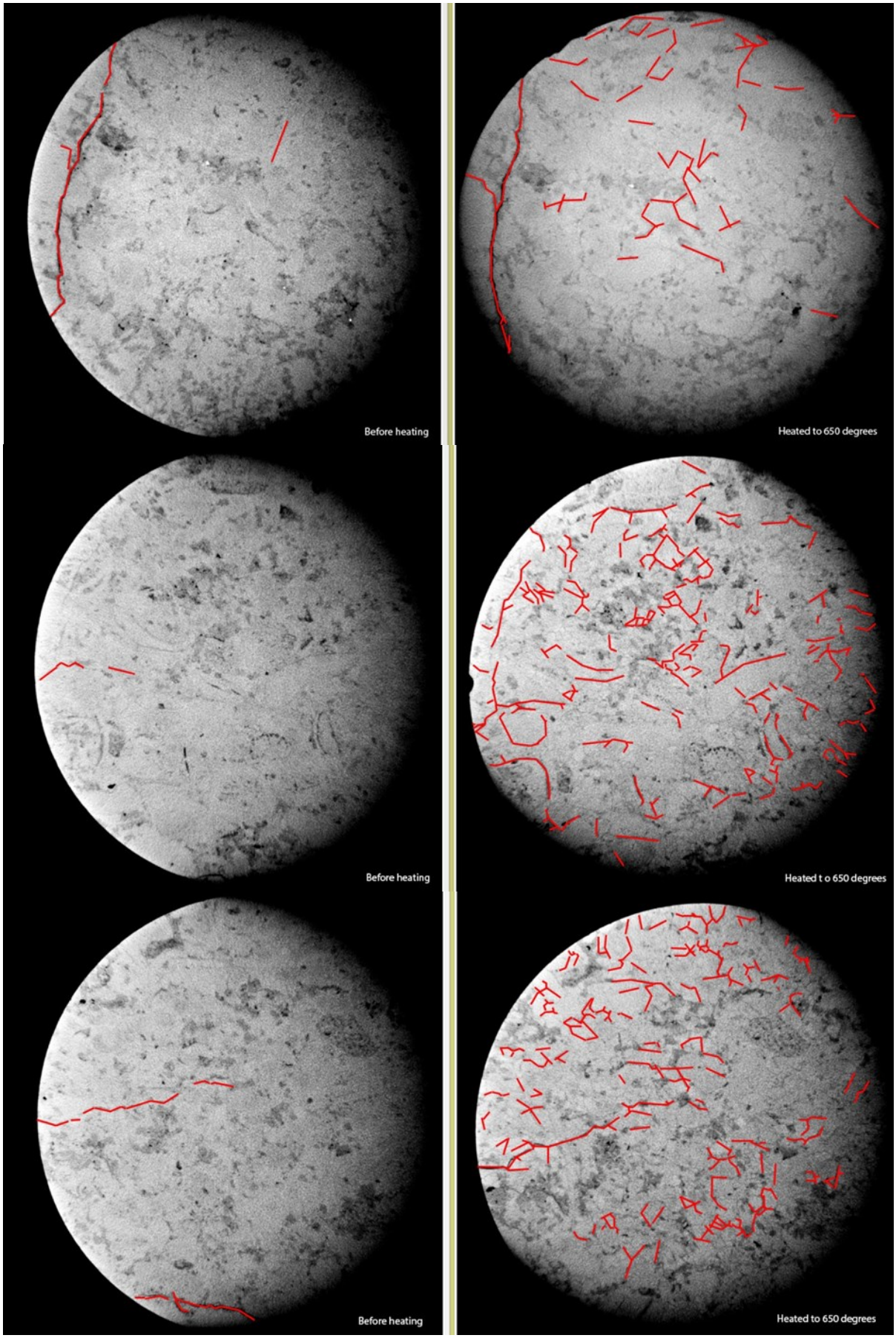
Before heating
Heated to 650 degrees
Before heating
Heated t o 650 degrees
Before heating
Heated to 650 degrees

7. The before and after CT pictures of the sample heated to 700 degrees. Fractures are marked in red.

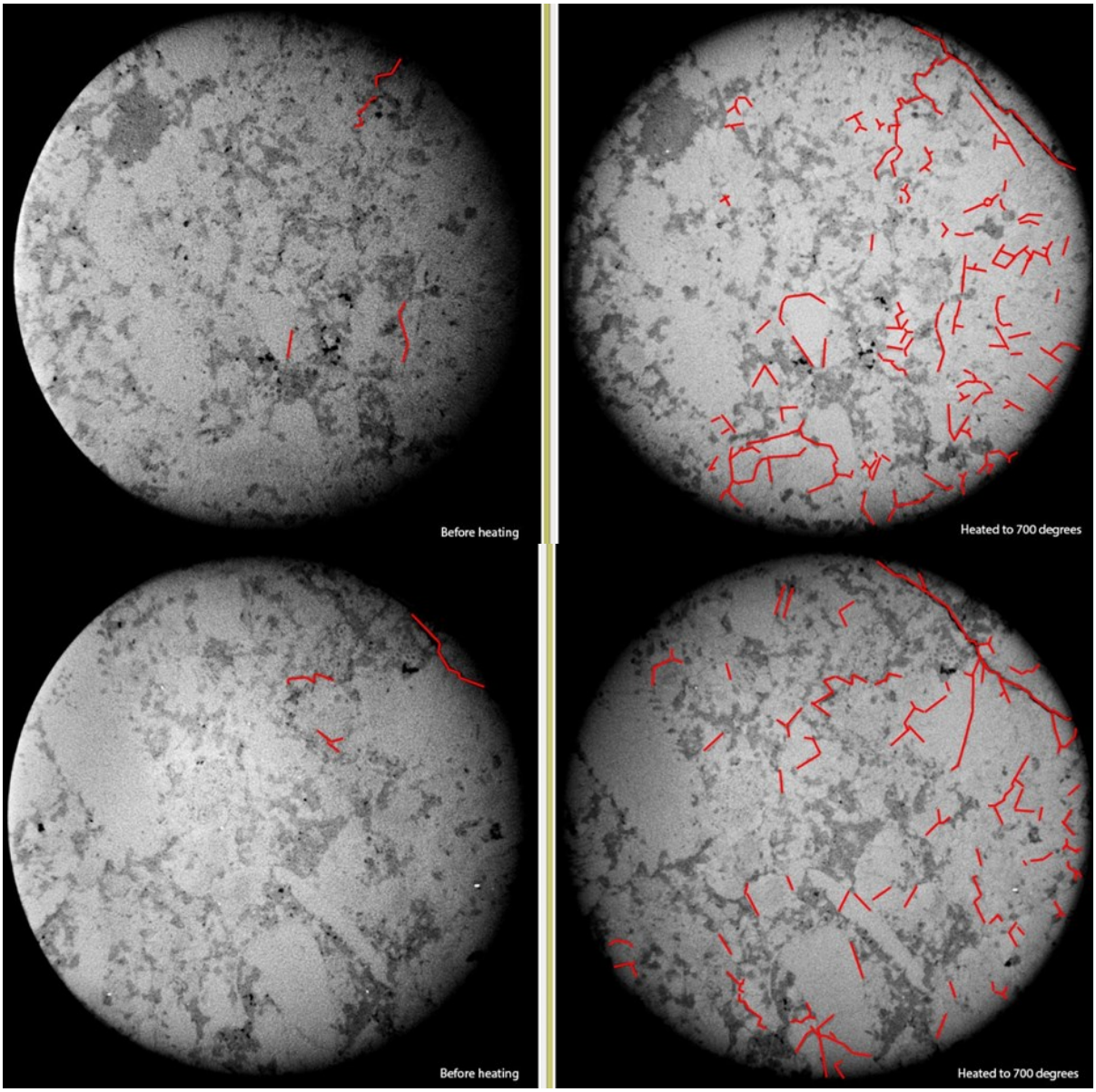

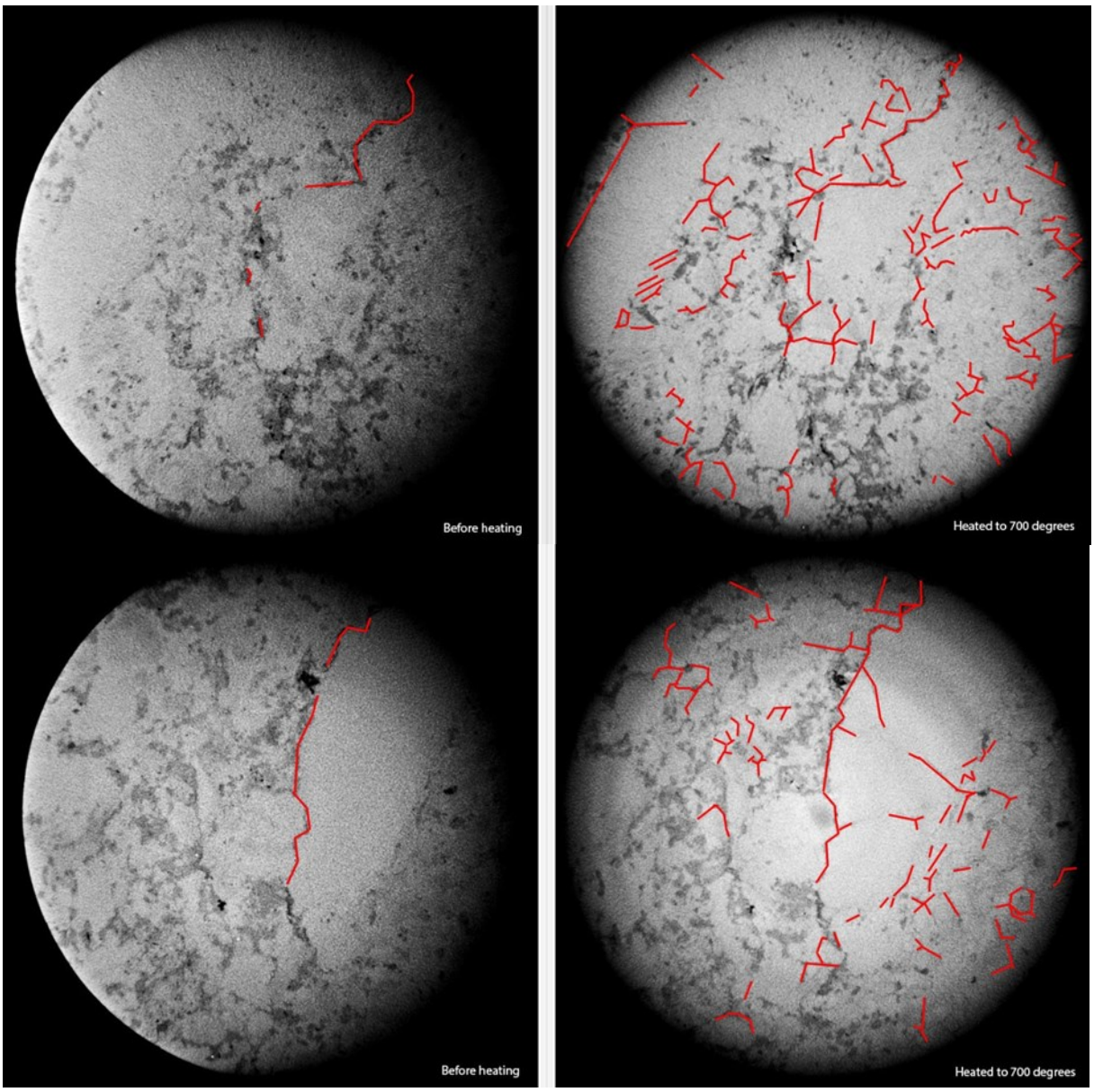
Before heating
Heated to 700 degrees
Before heating
Heated to 700 degrees

Tidigare skrifter i serien ”Examensarbeten i Geologi vid Lunds universitet”:

434. Vasilica, Alexander, 2015: Geofysisk karaktärisering av de ordoviciska kalkstensenheterna på södra Gotland. (15 hp)
435. Olsson, Sofia, 2015: Naturlig nedbrytning av klorerade lösningsmedel: en modellering i Biochlor baserat på en fallstudie. (15 hp)
436. Huitema, Moa, 2015: Inventering av föroreningar vid en brandövningsplats i Linköpings kommun. (15 hp)
437. Nordlander, Lina, 2015: Borrningsteknikens påverkan vid provtagning inför dimensionering av formationsfilter. (15 hp)
438. Fennvik, Erik, 2015: Resistivitet och IP-mätningar vid Äspö Hard Rock Laboratory. (15 hp)
439. Pettersson, Johan, 2015: Paleoekologisk undersökning av Triberga mosse, sydöstra Öland. (15 hp)
440. Larsson, Alfred, 2015: Mantelplymer - realitet eller *ad hoc*? (15 hp)
441. Holm, Julia, 2015: Markskador inom skogsbruket - jordartens betydelse (15 hp)
442. Åkesson, Sofia, 2015: The application of resistivity and IP-measurements as investigation tools at contaminated sites - A case study from Kv Renen 13, Varberg, SW Sweden. (45 hp)
443. Lönsjö, Emma, 2015: Utbredningen av PFOS i Sverige och världen med fokus på grundvattnet – en litteraturstudie. (15 hp)
444. Asani, Besnik, 2015: A geophysical study of a drumlin in the Åsnen area, Småland, south Sweden. (15 hp)
445. Ohlin, Jeanette, 2015: Riskanalys över pesticidförekomst i enskilda brunnar i Sjöbo kommun. (15 hp)
446. Stevic, Marijana, 2015: Identification and environmental interpretation of microtextures on quartz grains from aeolian sediments - Brattforsheden and Vittskövle, Sweden. (15 hp)
447. Johansson, Ida, 2015: Is there an influence of solar activity on the North Atlantic Oscillation? A literature study of the forcing factors behind the North Atlantic Oscillation. (15 hp)
448. Halling, Jenny, 2015: Inventering av sprickmineraliseringar i en del av Sorgenfrei-Tornquistzonen, Dalby stenbrott, Skåne. (15 hp)
449. Nordas, Johan, 2015: A palynological study across the Ordovician Kinnekulle. (15 hp)
450. Åhlén, Alexandra, 2015: Carbonatites at the Alnö complex, Sweden and along the East African Rift: a literature review. (15 hp)
451. Andersson, Klara, 2015: Undersökning av slugtestsmetodik. (15 hp)
452. Ivarsson, Filip, 2015: Hur bildades Bushveldkomplexet? (15 hp)
453. Glommé, Alexandra, 2015: $^{87}Sr/^{86}Sr$ in plagioclase, evidence for a crustal origin of the Hakefjorden Complex, SW Sweden. (45 hp)
454. Kullberg, Sara, 2015: Using Fe-Ti oxides and trace element analysis to determine crystallization sequence of an anorthosite -norite intrusion, Älgön SW Sweden. (45 hp)
455. Gustafsson, Jon, 2015: När började plattektoniken? Bevis för plattektoniska processer i geologisk tid. (15 hp)
456. Bergqvist, Martina, 2015: Kan Ölands grundvatten öka vid en uppdämning av de utgrävda dikena genom strandvallarna på Ölands östkust? (15 hp)
457. Larsson, Emilie, 2015: U-Pb baddeleyite dating of intrusions in the southeasternmost Kaapvaal Craton (South Africa): revealing multiple events of dyke emplacement. (45 hp)
458. Zaman, Patrik, 2015: LiDAR mapping of presumed rock-cored drumlins in the Lake Åsnen area, Småland, South Sweden. (15 hp)
459. Aguilera Pradenas, Ariam, 2015: The formation mechanisms of Polycrystalline diamonds: diamondites and carbonados. (15 hp)
460. Viehweger, Bernhard, 2015: Sources and effects of short-term environmental changes in Gullmar Fjord, Sweden, inferred from the composition of sedimentary organic matter. (45 hp)
461. Bokhari Friberg, Yasmin, 2015: The paleoceanography of Kattegat during the last deglaciation from benthic foraminiferal stable isotopes. (45 hp)
462. Lundberg, Frans, 2016: Cambrian stratigraphy and depositional dynamics based on the Tomten-1 drill core, Falbygden, Västergötland, Sweden. (45 hp)
463. Flindt, Anne-Cécile, 2016: A pre-LGM sandur deposit at Fiskarheden, NW Dalarna - sedimentology and glaciotectonic deformation. (45 hp)
464. Karlatou-Charalampopoulou, Artemis, 2016: Vegetation responses to Late Glacial climate shifts as reflected in a high resolution pollen record from Blekinge, south-eastern Sweden, compared with responses of other climate proxies. (45 hp)
465. Hajny, Casandra, 2016: Sedimentological study of the Jurassic and Cretaceous se-

quence in the Revinge-1 core, Scania. (45 hp)

466. Linders, Wictor, 2016: U-Pb geochronology and geochemistry of host rocks to the Bastnäs-type REE mineralization in the Riddarhyttan area, west central Berglsagen, Sweden. (45 hp)
467. Olsson, Andreas, 2016: Metamorphic record of monazite in aluminous migmatitic gneisses at Stensjöstrand, Sveconorwegian orogen. (45 hp)
468. Liesirova, Tina, 2016: Oxygen and its impact on nitrification rates in aquatic sediments. (15 hp)
469. Perneby Molin, Susanna, 2016: Embryologi och tidig ontogeni hos mesozoiska fisködlor (Ichthyopterygia). (15 hp)
470. Benavides Höglund, Nikolas, 2016: Digitization and interpretation of vintage 2D seismic reflection data from Hanö Bay, Sweden. (15 hp)
471. Malmgren, Johan, 2016: De mellankambriska oelandicuslagren på Öland - stratigrafi och faciestyper. (15 hp)
472. Fouskopoulos Larsson, Anna, 2016: XRF -studie av sedimentära borrkärnor - en metodikstudie av programvarorna Q-spec och Tray-sum. (15 hp)
473. Jansson, Robin, 2016: Är ERT och Tidsdomän IP potentiella karteringsverktyg inom miljögeologi? (15 hp)
474. Heger, Katja, 2016: Makrofossilanalys av sediment från det tidig-holocena undervattenslandskapet vid Haväng, östra Skåne. (15 hp)
475. Swierz, Pia, 2016: Utvärdering av vattenkemisk data från Borgholm kommun och dess relation till geologiska förhållanden och markanvändning. (15 hp)
476. Mårdh, Joakim, 2016: WalkTEM-undersökning vid Revingehed provpumpningsanläggning. (15 hp)
477. Rydberg, Elaine, 2016: Gummigranulat - En litteraturstudie över miljö- och hälsopåverkan vid användandet av gummigranulat. (15 hp)
478. Björnfors, Mark, 2016: Kusterosion och äldre kustdyners morfologi i Skälderviken. (15 hp)
479. Ringholm, Martin, 2016: Klimatutlöst matbrist i tidiga medeltida Europa, en jämförande studie mellan historiska dokument och paleoklimatarkiv. (15 hp)
480. Teilmann, Kim, 2016: Paleomagnetic dating of a mysterious lake record from the Kerguelen archipelago by matching to paleomagnetic field models. (15 hp)
481. Schönström, Jonas, 2016: Resistivitets- och markradarmätning i Ängelholmsområdet - undersökning av korrosiva markstrukturer kring vattenledningar. (15 hp)
482. Martell, Josefin, 2016: A study of shock-metamorphic features in zircon from the Siljan impact structure, Sweden. (15 hp)
483. Rosvall, Markus, 2016: Spår av himlakroppskollisioner - bergarter i nedslagskratrar med fokus på Mien, Småland. (15 hp)
484. Olausson, My, 2016: Resistivitets- och IP -mätningar på den nedlagda deponin Gustavsfält i Halmstad. (30 hp)
485. Plan, Anders, 2016: Markradar- och resistivitetsmätningar – undersökningar utav korrosionsförhöjande markegenskaper kring fjärrvärmeledningar i Ängelholm. (15 hp)
486. Jennerheim, Jessica, 2016: Evaluation of methods to characterise the geochemistry of limestone and its fracturing in connection to heating. (45 hp)

LUNDS UNIVERSITET

Geologiska institutionen
Lunds universitet
Sölvegatan 12, 223 62 Lund